G 867

EGG-92-02

**Idaho
National
Engineering
Laboratory**

EGG-EP-10557

An Integrated Approach to Reservoir
Engineering at Pleasant Bayou
Geopressured-Geothermal Reservoir

G. Michael Shook

 EG&G Idaho

December 1992

This document contains new concepts or the author(s) interpretation of new calculations and/or measurements; accordingly, EG&G Idaho, Inc. is required by the United States Government to include the following disclaimer:

An Integrated Approach to Reservoir Engineering at Pleasant Bayou Geopressured-Geothermal Reservoir

G. Michael Shook

Abstract

A numerical model has been developed for the Pleasant Bayou Geothermal-Geopressured reservoir. This reservoir description is the result of integration of a variety of data, including geological and geophysical interpretations, pressure transient test analyses, and well operations. Transient test analyses suggested several enhancements to the geologic description provided by University of Texas Bureau of Economic Geology (BEG), including the presence of an internal fault not previously identified. The transient tests also suggested water influx from an adjacent aquifer during the long-term testing of Pleasant Bayou; comparisons between transient test analyses and the reservoir description from BEG suggests that this fault exhibits pressure-dependent behavior. Below some pressure difference across the fault, it remains a no-flow barrier; above this threshold pressure drop the barrier fails, and fluid moves across the fault.

A history match exercise is presented, using the hypothesized "leaky fault." Successful match of 4 years of production rates and estimates of average reservoir pressure supports the reservoir description developed herein. Sensitivity studies indicate that the degree of communication between the perforated interval and the upper and lower sands in the reservoir (termed "distal volume" by BEG) impact simulation results very little, whereas results are quite sensitive to storage and transport properties of this distal volume. The prediction phase of the study indicates that Pleasant Bayou is capable of producing 20,000 STB/d through 1997, with the final bottomhole pressure approximately 1600 psi above abandonment pressure.

Introduction

The purpose of this report is to describe an integrated approach to reservoir engineering at the Pleasant Bayou geothermal-geopressured reservoir. A reservoir description was synthesized from all available data, including geologic and geophysical analyses and data from well operations (production rates, pressures, and results of pressure transient testing). The goal of this synthesis was to develop an accurate, internally consistent reservoir model for use in numerical simulation of Pleasant Bayou. The results of this approach and the numerical study are presented in the following sections.

The Pleasant Bayou fault block is located about 40 miles south of Houston, Texas, in Brazoria and Galveston counties. Based on work done at the University of Texas Bureau of Economic Geology (BEG) in the 1970s, this area was selected for testing by the Department of Energy (DOE) to assess the nation's geopressured-geothermal energy resource. Pleasant Bayou Well #1 (PB1) was drilled in 1978, but it was plugged back and recompleted as a disposal well because of hole instability problems. PB2 was offset from PB1 by 500 ft and was drilled to a depth of 16,500 ft.

Initial short-term testing of PB2 was conducted in 1979. A Reservoir Limits Test (Phase-1 testing) was conducted in 1980, and long-term testing was scheduled for 1981-1983 (Stevens and Clark, 1979). Numerous problems developed during the long-term testing, including wireline losses and scaling of the production tubing. Testing was suspended in 1983 when the production tubing string parted downhole.

Eaton Operating Company (EOC) took over well operations for DOE in 1985, and cleaned out and recompleted both PB2 and the disposal well PB1. The present configuration of the production well is given in Figure 1 (EOC, 1990). The Institute for Gas Technology (IGT) has been responsible for surface production measurements and has provided correlations for estimating bottomhole pressures from surface measurements.

Prior to the long-term testing that began in May 1988, BEG reviewed all previous geologic studies of the area (e.g., Bebout et al., 1980; Loucks et al., 1980; Ewing et al., 1984) and extended that work by focusing on the C-zone reservoir of the lower Frio formation (Hamlin and Tyler, 1988). The result of this effort was a comprehensive study of the geopressured sands. The study included detailed analyses of reservoir structure, sand thickness and continuity, faulting and reservoir boundaries, and estimates of reservoir volume.

PB2 was opened for production in late May 1988 and has produced approximately 25 million stock tank barrels (STB) of brine through September 1992. Two scale inhibitor "pills" have been injected into the

formation: the first prior to reopening the well in 1988 and a second in November 1989. Additional inhibitor has periodically been injected by pump at the surface as needed. The design of the inhibitor was based on work by Tomson et al. (1985) and has resulted in scale-free brine production the past four years.

Geologic and Geophysical Analyses

A contour map showing the structural top of the C zone of the lower Frio Formation (the geopressured sand) is shown in Figure 2 (from Hamlin and Tyler, 1988). The main structural features seen are two large growth faults that bound the reservoir on three sides (N, NE, and NW). The displacement across these faults ranges from 500 to 1,000 ft and is accompanied by large stratigraphic changes (Hamlin and Tyler, 1988). Pressure and fluid-chemistry analyses (Fowler, 1970) suggest that these faults act as impermeable boundaries within the Pleasant Bayou fault block. Reservoir closure south of PB2 has not been identified; therefore, distance to the southern boundary is to some extent a matter of conjecture. The nearest well to the south is more than 6 miles away; at that point, the C zone is 100% mudstone. Porosity pinchout is assumed to form this southern boundary; Bebout et al. (1978) have confirmed that porosity and permeability of reservoirs in the Pleasant Bayou fault block decrease to the southwest.

Within the Pleasant Bayou geopressured reservoir are numerous internal faults, identified on the basis of well control and seismic data. The data are relatively plentiful in the northern portion of the reservoir, but are extremely scarce south of the test well. In fact, we are not aware of any seismic data available from PB2 toward the south of the reservoir. None of the internal faults that have been mapped appear to be continuous across the fault block (Ewing et al., 1984) and therefore act only as partial barriers to flow.

The depositional environment of Pleasant Bayou reservoir sediment is that of a wave-modified deltaic sequence (Tyler and Han, 1982). The sandstones were deposited as distributary-channel and channel-mouth bars. Former channel axes are characterized by thick sandstone sequences separated by areas of lower sandstone content. The sand sequences are separated vertically by shales in the south and western portion of the reservoir, possibly reflecting bypassing of the main channel deposits to the northeast. A net sand isopach map, as developed by Hamlin and Tyler (1988), is given in Figure 3.

Another important parameter in developing an accurate reservoir description is sandstone continuity. Well logs and cores from throughout the C zone indicate that the sands are interbedded with numerous mudstones. By careful correlation of these interbeds, Hamlin and Tyler were able to

construct a series of cross sections and a fence diagram (Figure 4) of the C zone reservoir. The fence diagram displays a three-dimensional view of the reservoir and demonstrates the complexity of interbedding across the fault block. Only two of the mudstones appear continuous: the upper and lower reservoir boundaries are controlled by fairly thick (>50 ft) transgressive marine mudstones. Other, discontinuous mudstones appear within the reservoir; however, the sands can, in general, be considered as three persistent units: an upper, middle, and lower sand body. These three sand bodies come together as a single sand unit north of PB2, in the Chocolate Bayou area. Delineation into three sands at the test well, however, is obvious. Interbedding is most pronounced to the south and southwest of the well, again, possibly due to bypassing of the main sand-bearing channels to the northeast. These mudstones appear to be continuous from north and east of the test well to well beyond PB2 to the southwest and act as flow barriers between the sands in this region of the reservoir. Because these mudstones pinch out northeast of the well, the fluids in these upper and lower sands are not isolated from the test well. Their flow path is greatly increased, however.

In summary, an extensive review of the geology of Pleasant Bayou reveals several important features of the reservoir. Several internal faults have been identified from well control data and seismic imaging. These faults do not appear to be continuous across any portion of the sand; therefore, they do not act as flow barriers. While the reservoir sand approaches 200 ft in thickness in places, the reservoir is subdivided into three discrete sand bodies. These sands are separated from one another in the southern and western portions of the reservoir by shales. To the north and east, however, these mudstones pinch out, and the sand becomes a single hydrologic unit.

It is equally important to recall the spatial variation in reservoir information. The data are relatively plentiful north of PB2; however, no data exist within 6 miles of PB2 to the south. Transient test analyses can be useful in improving the reservoir description in this direction, as well as providing estimates of reservoir permeability, volume, and distance to boundaries. Results from these analyses are discussed below.

Transient Testing
PB2 has been subjected to pressure transient tests four times since being completed in 1979. Three of these tests included both drawdown and buildup tests. In addition to the "conventional" transient tests that have been conducted ("conventional" because downhole pressure gauges were used), four other periods are also amenable to transient test analysis. These additional pressure transients can be analyzed because of carefully controlled well operations. During two different periods, the production was maintained at a constant rate for an extended time. This allowed the

reservoir to enter pseudo-steady state conditions, which allows for estimates to be made of reservoir drainage volume. These flow periods were each followed by extended periods of shutin time, allowing for the estimation of average reservoir pressure. These analyses provided some of the most important - and controversial - data obtained concerning the reservoir.

Transient test analyses are detailed in Appendix A; composite test results are summarized in Table 1. The conventional tests gave excellent agreement on near-well properties for over 12 years of testing. Reservoir permeability is approximately 180 md, and well skin is near zero. The single exception to the low values of skin appears in the 1980 Reservoir Limits Test (RLT) buildup study (S = 5). No explanation is available for this anomalous value; however, it may have been a transient phenomenon associated with the recent well completion. Excluding this single test, values for skin range from -2 to 0.2. Other details of interest from these tests include a permeability barrier or transition at approximately 1,600 ft from the well and another at about 6,500 ft. Given the location of PB2 relative to sand deposition (see Figure 3), this nearer transition could reflect the reduced sand quality southwest of the well (the analyses suggest that the permeability decreases to ~110 md). The farther boundary appears likely to be a linear flow barrier according to transient test theory. Estimated distance to this fault and the distance to mapped faults from Figure 2 suggest the presence of a previously unmapped fault. One possible explanation is that the fault to the west of PB2 actually extends further south than is mapped (recall the lack of data in this area). The similarity between this proposed extension and the internal faulting north and east of PB2 should be noted from Figure 2.

Table 1.   Reservoir Properties from Transient Tests.

Permeability	180. md
Well Skin	0
Barriers and Transitions	Perm. transition to 110 md at 1600 ft No-flow barrier at 6500. ft.

Additional data obtained from transient tests include several estimates of reservoir volume and average reservoir pressure. Test results span several years and indicate a probable increase in reservoir volume between May 1990 and February 1992. The first pseudo-steady state drawdown (Oct. '89-May '90) results in a reservoir drainage volume of 26.3 billion ft^3. Average reservoir pressure estimated from transient test theory and from material balance considerations are in excellent agreement (10,345 psi vs. 10326 psi). Agreement between these two methods of analysis lends credence to the calculated reservoir volume and average reservoir pressure. When the buildup test was terminated, bottomhole pressure was about 40 psi below

P_{avg} and building up slowly. The slow pressure buildup is perhaps due to the irregular reservoir shape and partial barriers to flow.

Reservoir volume estimates from the second constant rate flow test indicate that drastic changes occurred prior to February, 1992. The analysis indicates a reservoir drainage volume of 43.6 billion ft^3, an increase of 66% over that estimated from the first test. Possible explanations for this apparent increase are given in Appendix A; however, it appears likely from available data that flow from an adjacent aquifer or other source has occurred. From the 1992 buildup data, the average pressure estimates from transient theory and material balance (using the new, larger volume) agree extremely well. Shutin pressure at the end of the buildup test is again quite slow, reflecting irregularity in the flow domain.

Therefore, in addition to yielding reservoir permeability, well skin, and distances to faults and permeability transitions, analysis of the pressure transients has suggested fluid recharge. This conclusion is regarded as rather controversial, and is not substantiated by any other data. For this reason, while the "conventional" transient test results (k, S, fault locations) are accepted at face value, the idea of fluid influx will be further tested numerically.

Petrophysical and Fluid Properties
Other data required in a simulation study includes petrophysical and fluid properties. Where laboratory data is unavailable, correlations are taken from the literature and used; otherwise the data is as reported in the cited studies.

The fluid produced from the Pleasant Bayou C zone is a 130,000 ppm brine containing dissolved gases. The salt is principally sodium chloride, but some divalent cations are also present. The dissolved gases are primarily methane (85%), with an appreciable quantity of carbon dioxide (10%). The produced gas-water ratio is about 24 standard cubic feet (SCF)/STB.

For purposes of the simulation study, two pseudocomponents were used to model the three major fluid constituents: "brine" and "methane." Use of pseudocomponents requires that the pure component properties be modified to account for the presence of other chemical species, a standard procedure in many types of enhanced oil recovery simulation studies (see, for example, Lake, 1989). In the following discussion, reservoir temperature is taken as 306° F, and average initial reservoir pressure is 10,716 psia at a reference datum of 14,100 ft subsea. These data are consistent with values measured prior to the 1988 multirate transient test (MRT).

Liquid viscosity as a function of salt content and temperature is taken from Perry's Handbook (1963); at reservoir temperature, the correlation

gives 0.28 cp. The effect of methane has been neglected in this calculation; however, the viscosity of saturated brine would differ by less than 3% (Ostermann et al., 1985). From Osif (1984), effects of methane on fluid compressibility also appear slight. For reservoir conditions of temperature, pressure, and salinity, fluid compressibility is 2.63×10^{-6} psi^{-1}.

Culberson and McKetta (1951) measured solubility of methane in fresh water at elevated temperature and pressure. Their correlation has been modified to account for changes in solubility as a function of salt content by Price et al. (1981). Using these correlations, we find that, at reservoir conditions, the maximum dissolved gas is approximately 32 SCF/STB. Given that the gas water ratio (GWR) is ~24 SCF/STB, the reservoir is assumed to be undersaturated with respect to methane. Furthermore, the pressure in the reservoir would have to fall below ~6,500 psi before free gas would begin to evolve from the brine. The presence of CO_2 in brine has the effect of increasing the bubble point pressure; however, this effect has been neglected from this calculation.

Brine density as a function of composition is given by Saad (1989), among others. Assuming the brine is a 130,000 ppm NaCl solution, density at surface conditions of pressure and temperature is 69 lb_m/ft^3. Density changes associated with elevated pressures and temperatures are accounted for in the formation volume factor, B_w. At average reservoir pressure and temperature, B_w = 1.049 rb/STB (McCain, 1979). While gas content will affect the formation volume factor, the error in neglecting gas in the calculation for B_w is less than one percent (McCain, 1979).

Hamlin and Tyler (1988) estimated reservoir porosity on the basis of core analysis of the perforated zone and on the basis of estimates derived from the inferred depositional environment. They interpreted the thicker sands to be better-sorted channel-mouth bars with a porosity similar to that of the perforated zone. Thinner sands, on the other hand, were interpreted as delta-front sands and thus show lower porosity. Given the lack of direct measurements in the C zone, we have adapted their estimates for use in our reservoir model and have assigned a porosity of 0.18 to the middle sand unit and a value of 0.09 to the upper and lower sand units.

Rock compressibility constitutes another important piece of information required for accurate simulations. Total system compressibility, c_t, is the sum of the brine compressibility, c_w, and pore volume compressibility, c_p. Pore volume compressibility is given as (Dake, 1978):

$$c_p = c_R/\varphi$$

where c_R, the rock compressibility, is obtained from uniaxial compression tests. Estimates for representative values of c_R have been obtained from

rock mechanics tests (Fahrenthold and Gray, 1985) and range from 3- to 6 x 10^{-7} psi^{-1}. Then, for φ = 0.18, $c_p \approx 1.67 - 3.33$ x 10^{-6} psi^{-1}; for the lower porosity sands $c_p \approx 3.33 - 6.67$ x 10^{-6} psi^{-1}. In both cases, we have used the mean value of the range for simulation purposes.

Petrophysical and fluid properties and summarized in Table 2.

Table 2. Summary of parameters used in Pleasant Bayou Model

Rock Properties		
Total pore volume		4.2 x 10^{10} ft^3
Pore compressibility	distal volume	2.5 x 10^{-6} psi^{-1} (top, bottom layers)
	proximal volume	5 x 10^{-6} psi^{-1} (middle sand)
Porosity	distal volume	0.09 top, bottom layers
	proximal volume	0.18 middle sand
Fluid Properties		
Bubble point pressure at T_R		6500. psia
Viscosity		0.28 cp
Standard density		69. lb/ft^3
Formation Volume factor		1.049 rb/STB
Initial Conditions		
Pressure at 14,100 ft SS		10,716. psia
Temperature		306. °F
Mole fractions: brine		0.9968
methane		0.0032 (24 SCF/STB brine)

Data Synthesis

The next step is to synthesize the data described above into a useful dataset for simulation. The simulator used in this study is TETRAD (Vinsome, 1990; Vinsome and Shook, 1992). TETRAD is a fully implicit, compositional finite-difference simulator validated against a variety of problem types, including oil and gas applications (Vinsome, 1990) as well as geothermal problems (Shook and Faulder, 1991).

One of the more helpful components of TETRAD is its graphical input and output capability. The geologic maps, Figures 2 and 3, were digitized and used directly in the input deck. A grid system was overlain, and the internal faults as mapped by BEG were "linearized" along grid blocks and entered in the input deck. These internal faults are considered impermeable barriers by assigning a zero transmissibility multiplier between two grid blocks separated by a fault. This could be easily modified by entering a nonzero multiplier. Fluid and petrophysical properties were entered in accordance with TETRAD requirements. In all cases, the models generated properties identical to those measured or estimated at reservoir conditions of pressure and temperature.

Near-well permeability input was 180 md, as estimated from the transient test analyses. The conventional transient tests also indicate a permeability transition to ~110 md at about 1,600 ft from the well. The isopach map (Figure 3) clearly shows that PB2 is on the edge of a delta lobe and that the lobe terminates just west of the well. If the termination of the lobe is associated with a transition to delta-front sands, it follows that the permeability would be reduced. This transition occurs approximately 1,600 ft from the well and appears to honor both the geologic description and transient test results; therefore, permeabilities are entered as large (180 md) for grid blocks "on lobes" and small (110 md) "off lobes." From core analysis, the top and bottom sands are assigned a permeability of 25 md (Morton et al., 1983). Vertical permeability has been assigned a value of 1/10 of the horizontal permeability everywhere.

The fault postulated on the basis of transient tests at approximately 6,500 ft from the well is shown as an extension of the mapped fault west of PB2 to the southern boundary. This fault is considered impermeable; therefore, the connected pore volume is reduced from 41.7 billion ft^3 (total from planimetering BEG maps) to 23.4 billion ft^3. This reduced pore volume is approximately equal to the reservoir volume estimated in the first constant rate flow test (V_p = 26.3 billion ft^3), supporting the validity of this reservoir description during the 1988-1990 flow period. Furthermore, the total pore volume of 41.7 billion ft^3 is similar to the drainage volume estimated from the second flow test (V_p = 43.6 billion ft^3). The similarity in these volume estimates suggests that the integrity of the postulated fault may be responsible for the reservoir behavior identified in the transient test analyses. However, no mechanism for volume change or fluid influx is included in the initial simulation work.

Also from the transient tests, well skin was zero; however, inflow performance calculations suggest the presence of turbulent flow at rates in excess of 16,500 STB/d. On the basis of this, a pseudoskin (Dake, 1978) was implemented in TETRAD. The resulting productivity index (PI) for the well is given as:

$$PI = PI^o - 0.2275[q - 16500]^{1/3}$$

Figure 5 shows the "working map" generated by TETRAD's preprocessor. A grid of 41 x 22 x 6 was used in the study; however, the grid was refined nine-fold within the 3 x 3 subgrid at the well. The vertical mesh was manipulated such that the middle sand had a thickness of 62 ft at PB2, consistent with observed data. Transmissibility multipliers of zero were used to simulate the shales separating the three sands in the southwestern portion of the field. The length of these shale breaks is consistent with the fence diagram from BEG (Figure 4).

Simulation Studies

In order to successfully predict reservoir response to future exploitation, a history match exercise was first undertaken. "Day 1" was taken as Jan. 1, 1988. Prior to the start of the 1988 MRT, bottomhole pressure was recorded as 10,716 psi, corrected to the average depth of 14,100 ft subsea. Daily production data (rates and bottomhole pressures) reported by EOC were used in the history match, with bottomhole pressure being used as the well constraint, and brine production rate as the match variable.

Figure 6 shows the comparison between simulated and observed production rates through April 1992. Several observations can be made from this figure. With the exception of a 3- to 4-day period (at about 250 days), at early times we are able to obtain an excellent match of the observed production rate. At later times (t > 1,200 days, early 1991), the predicted rate deviates from the observed, consistently underpredicting production. Further analysis of the output suggests the cause of this failure to predict correctly at later times.

From transient test analysis and material balance calculations (detailed in Appendix A), average reservoir pressure at t = 881 days (after the June-July 1990 pressure buildup test) is estimated to have fallen by approximately 390 psi from its initial value. From TETRAD, ΔP = 385 psi, which is an excellent agreement between transient test, material balance, and numerical estimates. However, the pressure drop at t = 1,508 days (April 1992) is given as ~500 psi from transient tests and material balance considerations; TETRAD gives 770 psi. Furthermore, the transient tests suggest that the reservoir volume has increased between these dates by ~66% – from 26.3 billion to 43.6 billion ft^3. This increase has not been accounted for in this first simulation. If such an increase did in fact occur, this simulation could sustain neither the reported production rate nor the average reservoir pressure. This error in predicted rates and average reservoir pressure again leads (as did transient test analyses and material balance calculations) to the idea of influx of brine from a previously unconnected source.

By considering the similarity in volume estimates as determined from the geologic studies and transient test analyses, an initial estimate of the source of the additional fluid is obvious. Results of the two pseudo-steady state transient tests suggest that the reservoir increases in volume from 26.3 to 46.3 billion ft^3 between July 1990 and April 1992. The smaller of these two values agrees well with the volume in contact with PB2, as long as the new fault does not leak; the larger volume is virtually identical with the total pore volume of the Pleasant Bayou reservoir, as mapped by BEG (Hamlin and Tyler, 1988). This suggests that the fault postulated herein acts as a pressure-dependent flow barrier. For a given

pressure differential across the fault, the fault acts as a barrier to flow. Above this threshold, however, fluid is able to flow. Pressure-dependent behavior of this sort has been identified in the past (e.g., Hunt, 1990; Powley, 1987) and is the subject of ongoing research (Anderson et al., 1991).

The model implemented in TETRAD to account for this behavior is a simple, linear relationship between pressure drop across the fault and transmissibility at the fault face. For a sufficiently small pressure drop, the transmissibility at the fault face is zero; and no flow exists. This is the case envisioned early in the producing life at the Pleasant Bayou reservoir. As the pressure drop exceeds a threshold value, transmissibility at the fault face increases linearly with ΔP; and fluid can move from one side to the other. A non-zero transmissibility at this fault allows the entire reservoir volume to be drained by the well, as estimated from the 1991-1992 long-term drawdown analysis. This increase in volume also lengthens the time required for the reservoir to enter pseudo-steady state, as indicated by the increase in t_{pss} between the 1990 and 1992 constant-rate tests.

The model used in this study is shown in Figure 7. No attempt was made to adjust the minimum threshold pressure drop. Anderson (1992) suggests that this minimum should be approximately equal to maximum horizontal stress; this value has been approximated as 1,000 psi, slightly less than one-third of the total effective stress.

A second history match attempt was made with this adjusted reservoir description. Results from this run are shown in Figure 8. This figure clearly shows a much improved match of production through April 1992 (t = 1,550 days). Average reservoir pressure predicted at the end of the 47-day buildup ending in April 1992 is 10,233 psi – this time in excellent agreement with transient test analysis (P_{avg} = 10,243 psi) and material balance (P_{avg} = 10207 psi). Based on agreements between simulated and observed production rates and reservoir pressures, we conclude that the reservoir description detailed above accurately represents the important aspects of the Pleasant Bayou reservoir.

A final point of interest concerns the rate of fluid influx across the "leaky fault." Recharge rates into geopressured reservoirs have been discussed by a variety of authors, and values range from 2×10^{-3} ft/d (Negus-de Wys, 1992) to as large as 0.1 ft/d (Anderson, 1991). These ranges reflect postulated recharge behavior, which can vary from a low, constant rate of recharge to a relatively large, episodic amount of recharge. Calculations based on TETRAD results suggest that the superficial (Darcy) velocity across the leaky fault is approximately 0.1 ft/D, at the upper limit of postulated influx rates. Anderson (1992)

further states that pressure-dependent faults close as the pressure differential across the fault declines. This behavior has not been identified at Pleasant Bayou through the history match exercise; however, insufficient long-term flow data exist to determine whether this would occur.

Sensitivity Studies

Having obtained good agreement between simulated and observed behavior at Pleasant Bayou, we now undertake to study the effects of uncertainty in our reservoir model. Transient tests have identified effective reservoir properties in the middle sand, and we will continue to assume that these properties are accurate. Reservoir properties of the upper and lower sands, however, were obtained from single point measurements (core analyses) and may well not be representative of the sand properties. For this reason, a limited sensitivity study was undertaken to evaluate the effect of error in the reservoir model.

Reservoir properties varied include permeability and porosity of the upper and lower sands, vertical permeability, and extent of the shale barrier separating the three sands. Sensitivity runs are summarized in Table 3 and are presented graphically in Figures 9 and 10. Figure 9 shows that neither shale extent nor vertical permeability has much effect on simulation results. The lack of significance of vertical permeability is somewhat intuitive, given the cross-sectional area open to flow. Insensitivity to shale length, on the other hand, is somewhat surprising. In Run PBSH1, the shale is extended nearly 5 miles further than suggested by BEG (see Figure 4) and into an area with sufficient well control. This extension exceeds a maximum possible shale length and yet impacts the simulation results only minimally.

Table 3. Summary of Sensitivity Runs.

Run #	Parameter Changed from Base Case
PBK1	Permeability in upper, lower sands increased to 110 md.
PBSH1	Shales extended additional 25000 ft. NE of PB2
PBKSH	Both changes noted above together (perm and shale length increased)
PBKV1	Vertical permeability = horizontal permeability everywhere
PBP1	Porosity in upper, lower sands increased to 0.18

Transport and storage properties of the upper and lower sands have much greater impact on simulation results, as shown in Figure 10. The

similarity in results between PBK1 and PBKSH again points to the insensitivity to the areal extent of the shale; however, changes in either permeability or porosity of the upper and lower sands result in drastic changes in predicted behavior. Obviously, the analysis concerning depositional environment and (therefore) sand property estimates made by BEG were extremely useful in developing a good reservoir model. In the absence of such an analysis, extensive history match simulations would have been required to establish reasonable properties for these sands.

Model Predictions

The final portion of this study involves predicting how the Pleasant Bayou geopressured reservoir would respond to future exploitation. Long-term exploitation is simulated in the following fashion. Bottomhole pressure is constrained to be at least 7,000 psi, and the brine production rate is no greater than 20,000 STB/d. The bottomhole pressure constraint corresponds to approximately 500 psi minimum surface pressure, assuming a hydrostatic head of fluid. The production limit is close to the limit of allowable production rate without sand production problems. The simulation proceeds as follows. As long as the brine production rate can exceed 20,000 STB/d, bottomhole pressure is increased such that the rate is 20,000 STB/d. As reservoir pressure declines, the bottomhole pressure also falls in order to maintain this production rate. Finally, the bottomhole pressure falls to its minimum, and 20,000 STB/d can no longer be maintained. At this point, the production rate will begin to decline, and bottomhole pressure remains constant. The prediction time extends through 1997; therefore, simulated production life of the reservoir is 10 years (1988-1997).

Bottomhole pressures vs. time for this prediction run is given in Figure 11. Throughout the prediction phase, the brine production rate is maintained at 20,000 STB/d. As can be seen from this figure, PB2 can maintain production rates of 20,000 STB/d into the 21st century. At the end of this simulation (end of 1997), predicted bottomhole pressures are still 1,600 psi above abandonment pressure. However, it should also be noted that this simulation does not assume that the leaky fault will close. Should the recharge (influx) path change, as suggested by Anderson (1992), these predictions would, of course, require modifications. As was noted, there does not appear to be sufficient information regarding the behavior of the leak to determine its future behavior.

In fact, it is recognized that PB2 is scheduled to be shut-in in late 1992. Buildup behavior is very sensitive to production just prior to shutin; therefore, the pressure response cannot be predicted with any accuracy at this time. The final pressure buildup will be examined when these data become available in FY 1993.

Summary and Conclusions

This report summarizes the development of a reservoir model for predicting behavior of the Pleasant Bayou geopressured-geothermal reservoir. The model incorporates all data available from a variety of sources, including geologic and geophysical information, transient test analyses, and reported production information. By incorporating these diverse data sources, an internally consistent dataset was developed. This reservoir model honors all of the available data without undue simplifications or assumptions, and incorporates "leaky fault" behavior not previously identified at Pleasant Bayou. Based on this approach, the following specific conclusions are made:

An excellent match of production history was obtained through February 1992 using the model developed herein.

On the basis of transient analyses and numerical studies, an additional geologic feature was incorporated into the BEG model. The pressure-dependent fault is located in an area in which no data are available and therefore the fault cannot be rigorously validated. However, no less than three transient analyses indicate the presence of a fault not indicated on the BEG maps, and additional evidence suggests fluid recharge at Pleasant Bayou. Estimates of increased fluid volume and average reservoir pressures all suggest that only part of the sand was initially in communication with PB2 until sometime in 1991. No available evidence contradicts the hypothesized recharge.

Model predictions are very sensitive to errors in properties of the upper and lower sands. On the other hand, the extent of the shale barrier has little influence on reservoir performance. This is likely due to the large surface area over which the three sands communicate in the northeast portion of the field.

On the basis of the history match exercise, PB2 is capable of producing more than 20,000 STB/d of brine for at least 10 years of production. This conclusion assumes that the fault that has opened remains open. It may also represent a minimum production life, in that other recharge may occur as the reservoir is depleted.

An additional analysis is planned to evaluate and model the pressure buildup when PB2 is shut in.

Acknowledgments

Figure 1. PB2 Configuration. From EOC, 1990

126'   ◄──── 25" - DRIVE PIPE

         24" HOLE: 0' TO 1,415'

1,395'   ◄──── 20" H-40 & K-55 STC CASING

         5-1/2" P-110 TUBING W/ NEW VAM MS/ATAC

         17-1/2" HOLE: 1,415' TO 8,517'

8,487'   ◄──── 13-3/8" S-95, L-80 & N-80 STC CASING

         12-1/4" HOLE: 8,517' TO 14,343'

         ◄──── 13,952' TOP BROWN 2-5 PERMANENT PACKER

         ◄──── 13,991' TOP 9-5/8" x 7" HANGER
         ◄──── 14,174' TOP OF CEMENT
14,284' ◄──── 9-5/8" S-105 & S-95 BUTT CASING

         ◄──── 14,644' TO 14,704': PRODUCTION PERFORATIONS
         ─── WIRELINE & TOOL BELOW 14,705'

         ◄──── 15,475' PREVIOUS CLEANED OUT T.D.

         8-3/4" HOLE: 14,343' - 16,500'

16,465' ◄──── 7" P-110 SHFJ LINER: 14,015' TO 16,465'
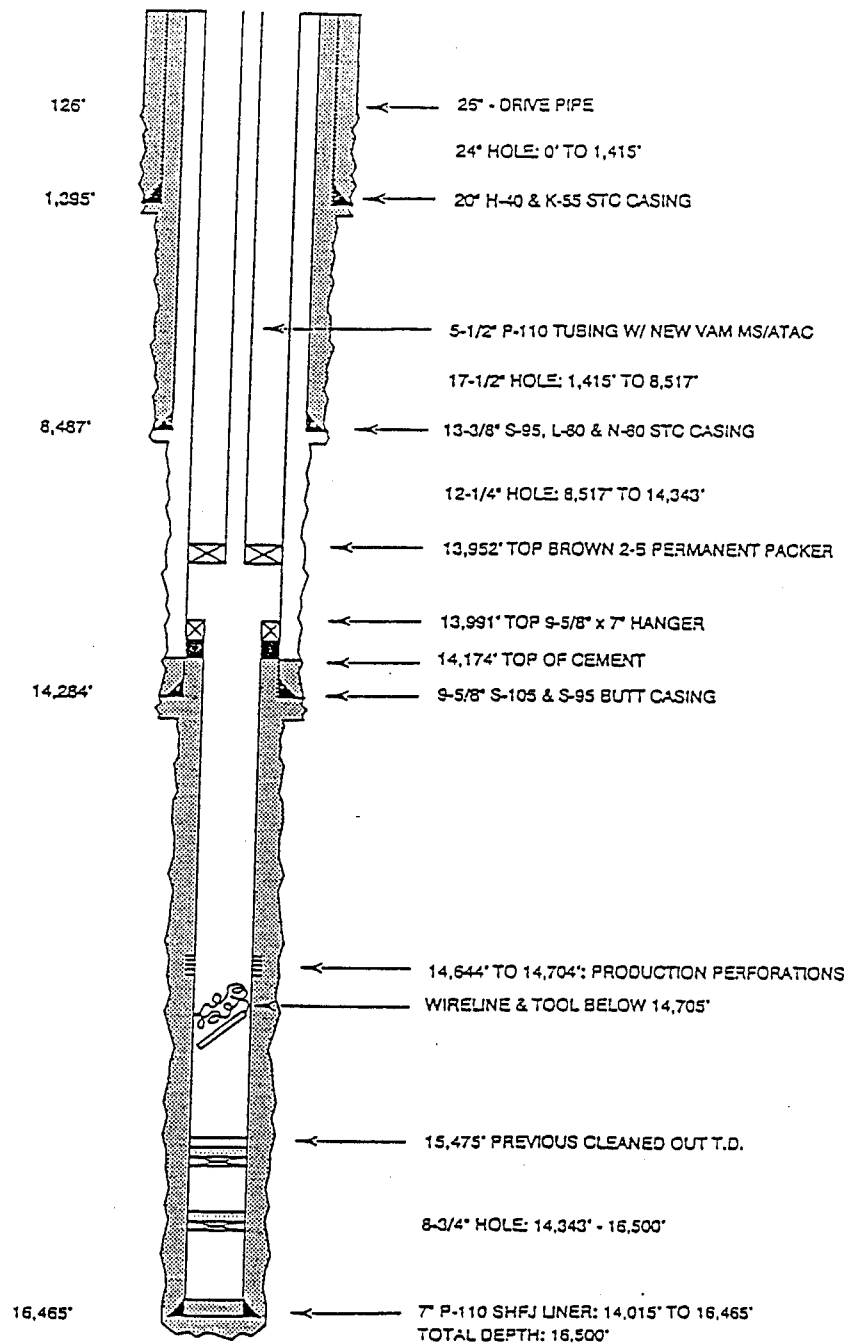   TOTAL DEPTH: 16,500'

Figure 2. Structure Map, Top of C Zone, Pleasant Bayou Reservoir.
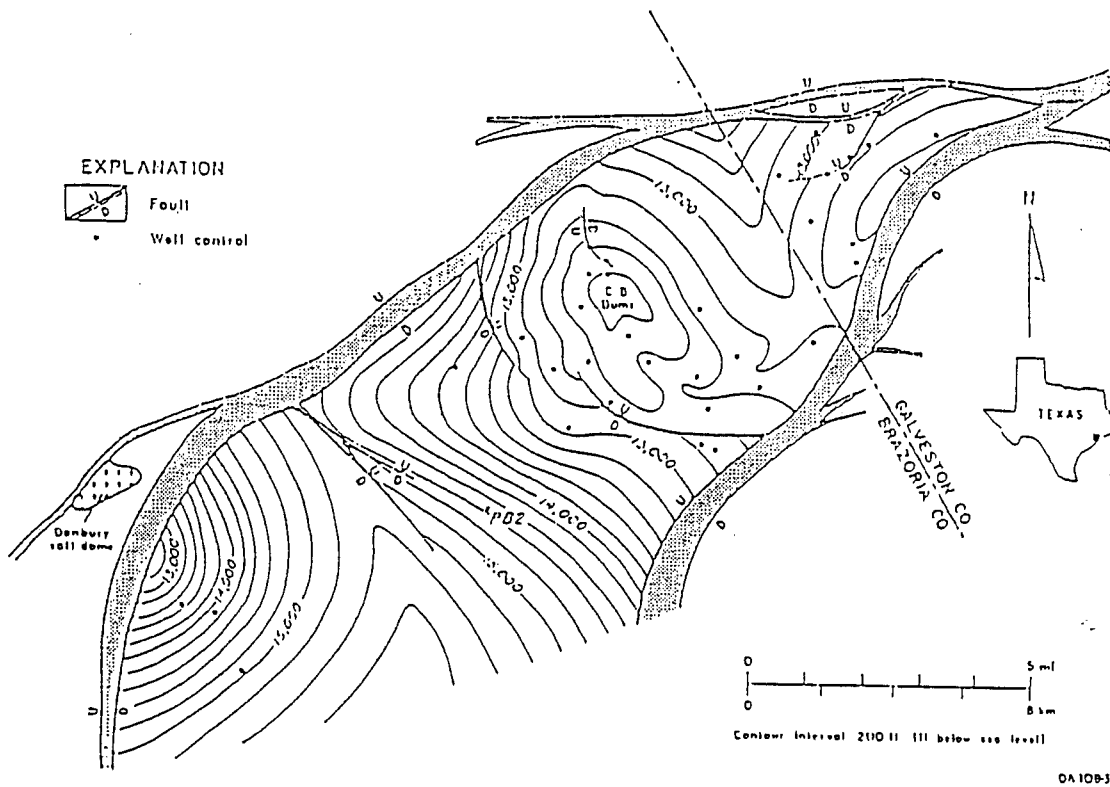From Hamlin and Tyler, 1988.

Figure 3. Isopach of C Zone, Pleasant Bayou Reservoir.
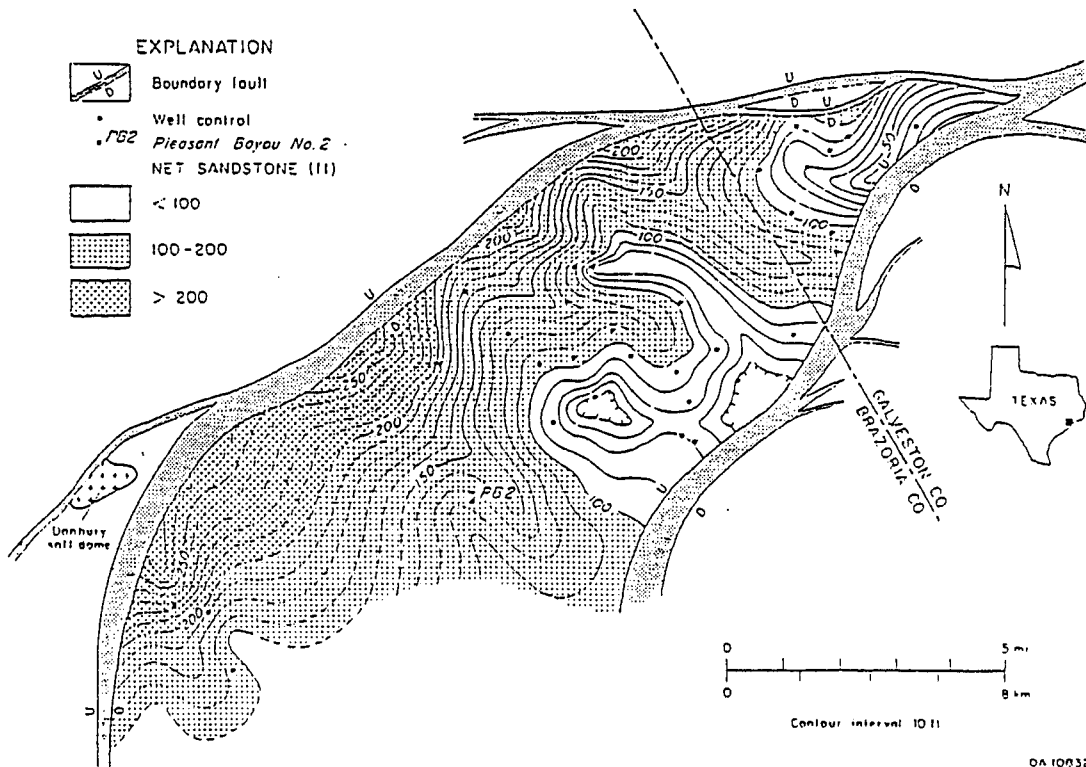From Hamlin and Tyler, 1988.

Figure 4. Fence Diagram Showing Sand/Shale Continuity,
Pleasant Bayou Reservoir.   From Hamlin and Tyler, 1988.

EXPLANATION

Sandstone

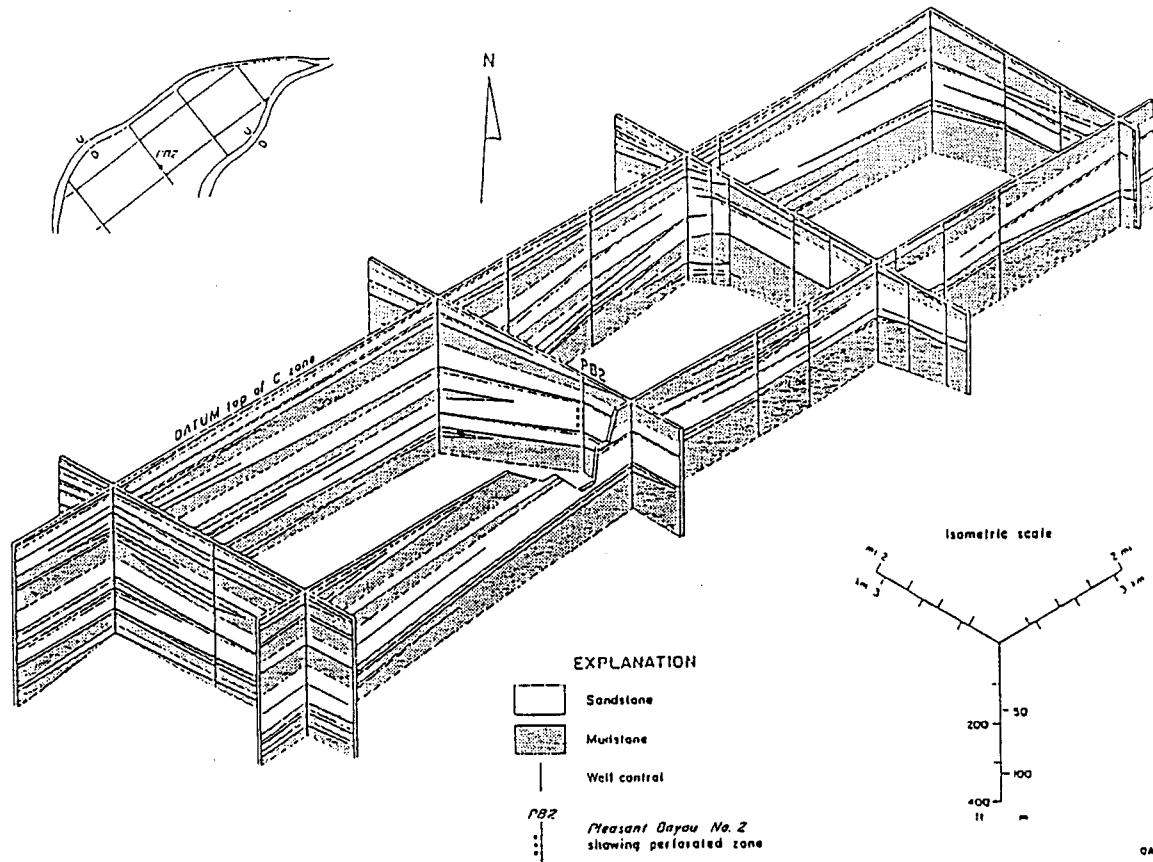Mudstone

Well control

PB2   Pleasant Bayou No. 2
       showing perforated zone

Isometric scale

GA10640

Figure 5. Working Map of Pleasant Bayou Reservoir, Plan View.

PB2

——— Faults per BEG Model   ⌄⌄⌄ New Fault   ▨▨▨ Null Blocks
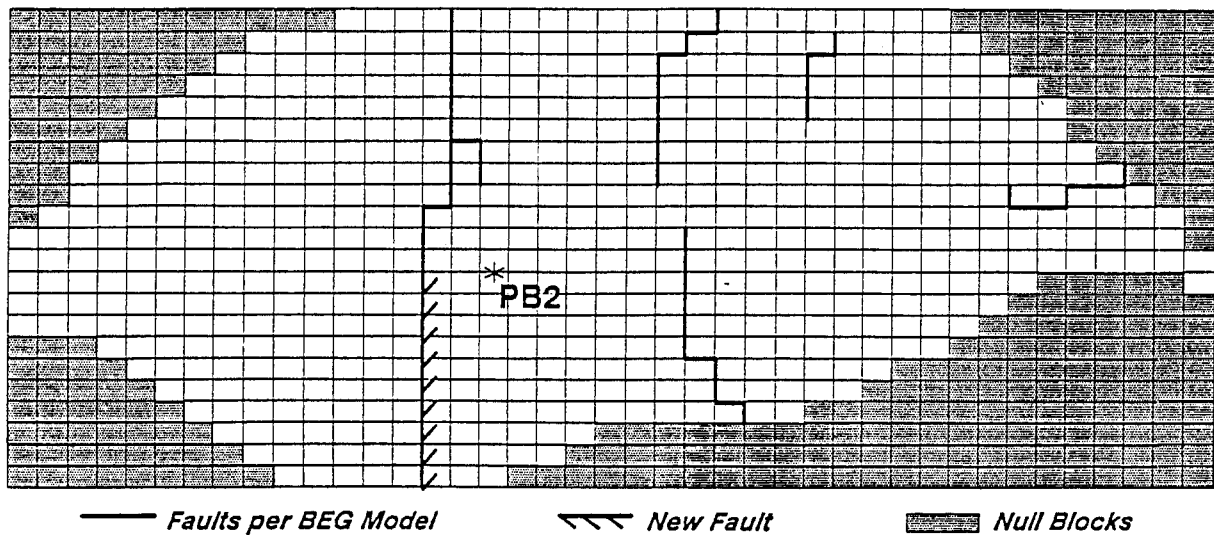
Figure 6. New fault acts as no-flow barrier. Note the consistent under-estimation of rate at late (t > 1100 days) times.

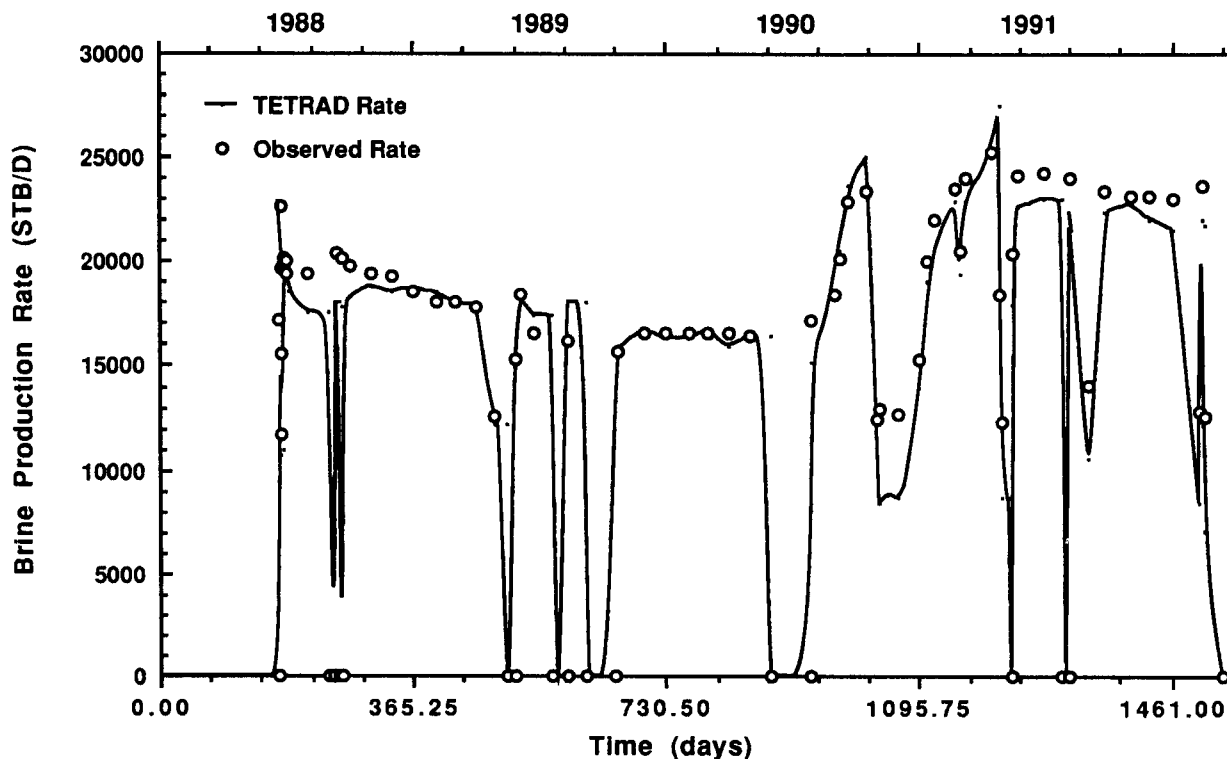**Figure 7. Schematic of pressure-dependent fault. Fault is no-flow until pressure exceeds a threshold, and increases linearly to a maximum.**
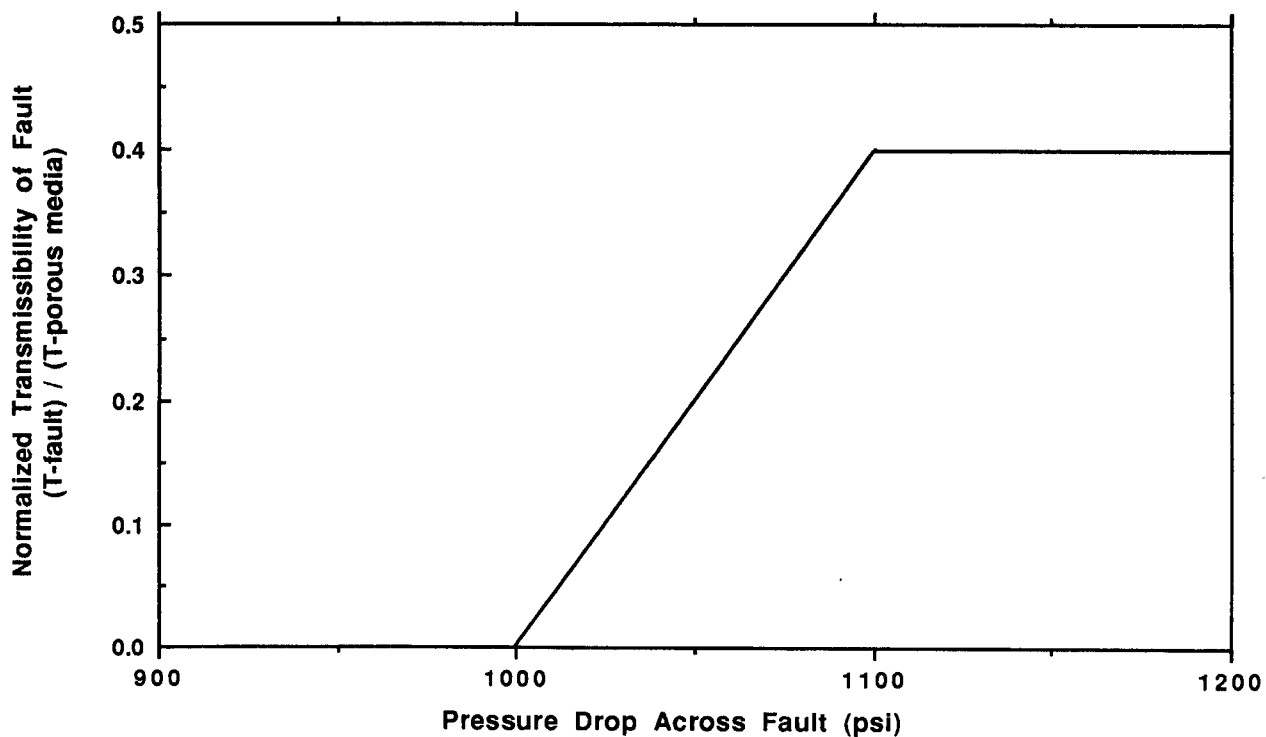
Figure 8. History match of observed production. New fault leaks for pressure differentials greater than 1000 psi.
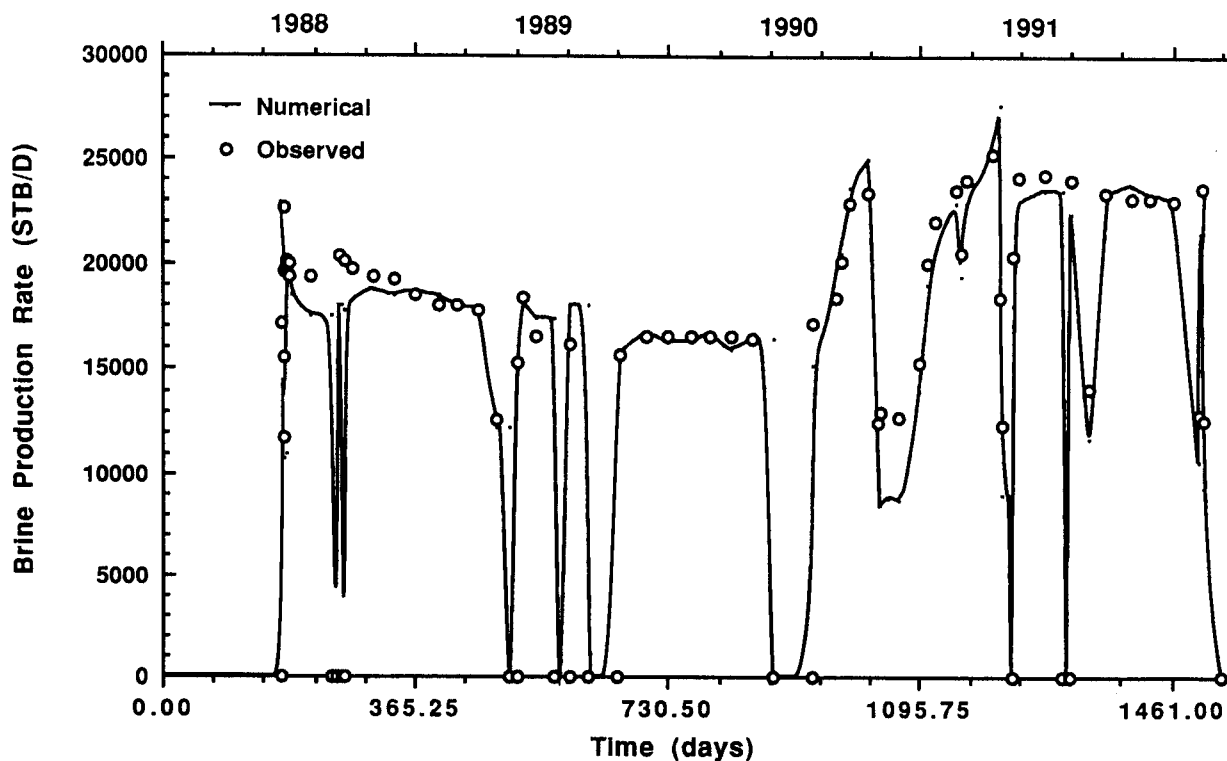
Figure 9. Sensitivity study results show vertical permeability and shale extent affect results very little, runs compare well w/ PBBC.

Figure 10. Changes in flow and storage properties of the upper and lower sands affect history match greatly.

Figure 11. Predicted bottomhole pressure vs. time for PB2. Brine production rate remains at 20,000 STB/D through 1997.

Nomenclature

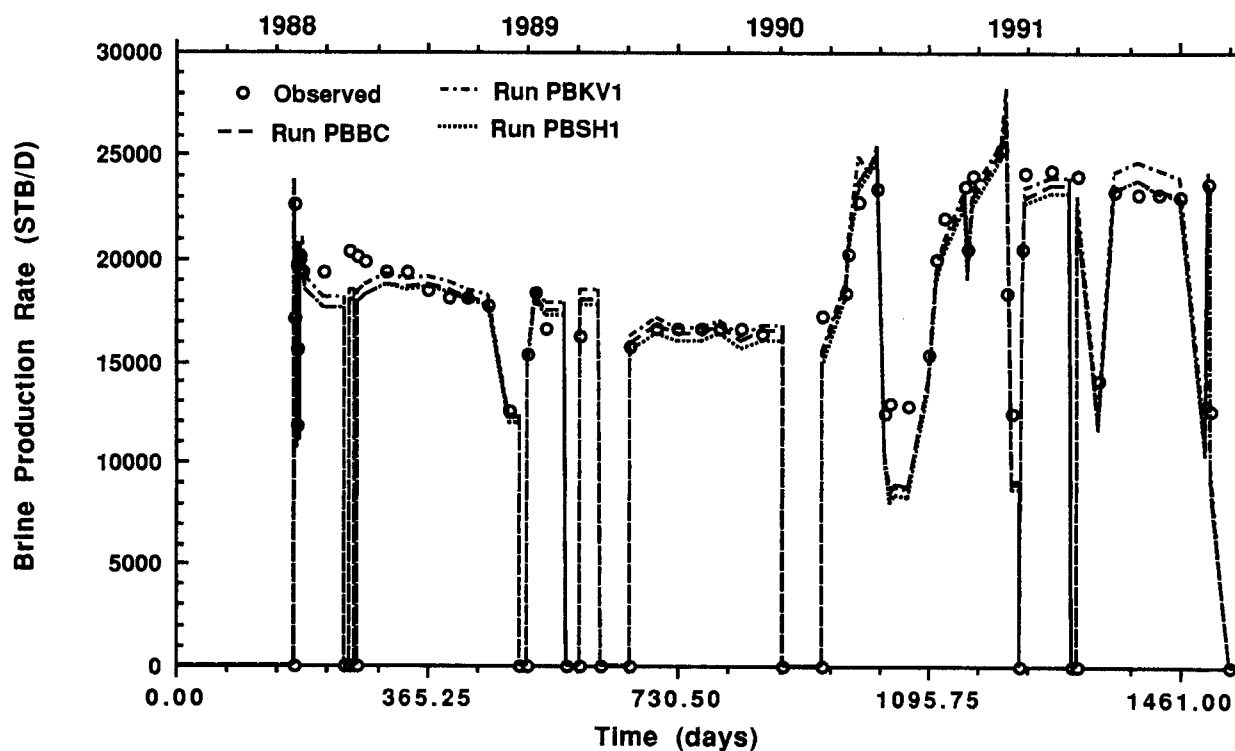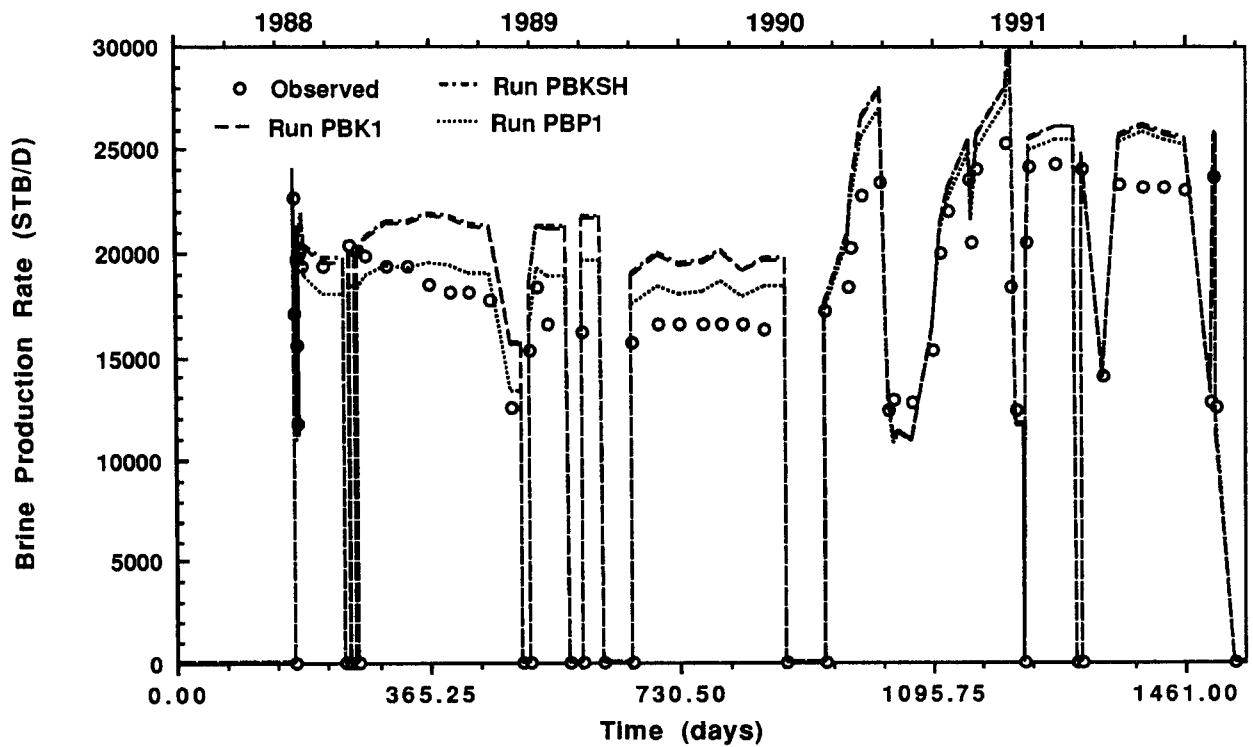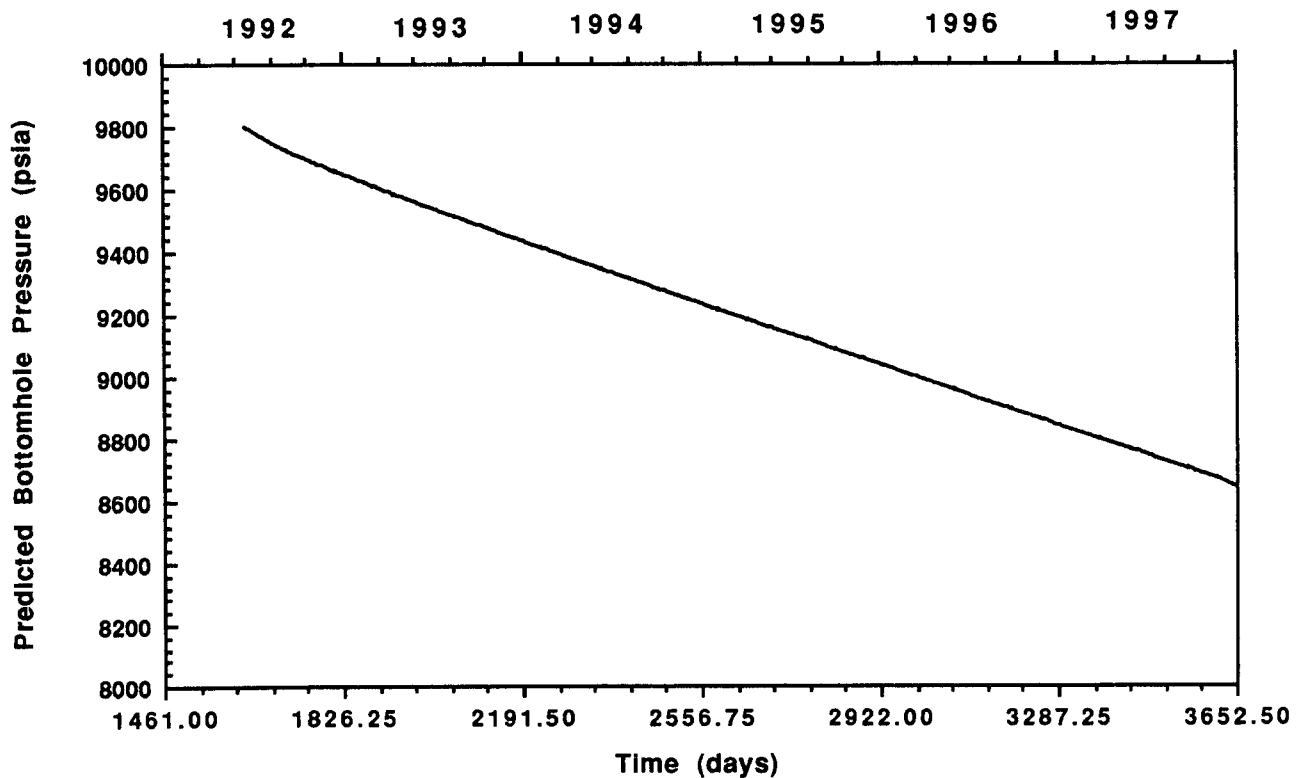|	
B_W	Formation Volume Factor [=] res. volume/vol. at 60° F, 14.7 psia
c_p	Isothermal pore space compressibility [=] psi^{-1}
c_R	Isothermal compressibility of rock [=] psi^{-1}
c_t	Total system isothermal compressibility $(c_W + c_p)$ [=] psi^{-1}
c_W	Isothermal compressibility of brine [=] psi-1
C zone	Geopressured sand, lower Frio Formation
GWR	Gas-water ratio
h	Thickness of sand [=] ft
k	Permeability [=] md
L_x	Distance to fault or permeability transition [=] ft
m	Slope of transient test pressure-time line, units vary
md	milli-darcy
MRT	Multi-rate test
P_{avg}	Average reservoir pressure [=] psia
PB1	Pleasant Bayou Well #1
PB2	Pleasant Bayou Well #2
P_{DMBH}	Mathews-Brons-Hazebroek dimensionless pressure
PI	Productivity index of a well [=] STB/d/cp/psi
pss	pseudo-steady state
P_{wf}	Flowing well pressure [=] psia
P_{ws}	Shutin well pressure [=] psia
Q	Cummulative production [=] STB
q	Volumetric production rate [=] STB/d
q_N	Rate of step N in multistep rate test [=] STB/d
rb	reservoir barrels = 5.615 ft^3 at reservoir conditions of P,T
RLT	Reservoir Limits Test
r_w	Wellbore radius [=] ft
S	Well skin [=] dimensionless
SCF	Standard cubic feet [=] ft^3 at 60. F, 14.7 psia
STB	Stock tank barrels = 5.615 ft^3 at 60. F, 14.7 psia
t	Time [=] days
tp	Length of production time determined as Q/q [=] hrs
tpss	Time required for onset of pseudo-steady state [=] hrs
t_{DMBH}	Dimensionless production time used in MBH buildup theory

Greek

μ	viscosity [=] cp
φ	porosity [=] void volume/bulk volume
Δ	Difference operator

REFERENCES

Anderson, R. N., L. M. Cathles, III, and H. R. Nelson, Jr., 1991, "'Data Cube' Depicting Fluid Flow History in Gulf Coast Sediments," *Oil and Gas Journal*, November 4, 1991.

Anderson, R. N., 1992, Personal Communication.

Bebout, D. G., R. G. Loucks, and A. R. Gregory, 1980, "Geological Aspects of Pleasant Bayou Geopressured-Geothermal Test Well, Austin Bayou Prospect, Brazoria County, Texas," *Proceedings, Fourth Geopressured Geothermal Energy Conference*, The University of Texas at Austin, Center for Energy Studies, M. H. Dorfman and W. L. Fisher, eds., 1980, pp. 11-45.

Bebout, D. G., R. G. Loucks, and A. R. Gregory, 1978, "Frio Sandstone Reservoirs in the Deep Subsurface along the Texas Gulf Coast: Their Potential for Production of Geopressured Geothermal Energy," *The University of Texas at Austin, Bureau of Economic Geology Report of Investigations, 91*, 1978.

Culberson, O. L., and J. J. McKetta, Jr., 1951, "Phase Equilibria in Hydrocarbon-Water Systems: IV - Vapor-Liquid Equilibrium Constants in the Methane-Water and Ethane-Water Systems," *Trans. Society of Petroleum Engineers of the AIME, 192, 1951*, pp. 297-300.

Dake, L. P., 1978, *Fundamentals of Reservoir Engineering*, Elsevier Scientific Publishing Co., Amsterdam, The Netherlands, 1978.

Earlougher, R. C., 1978, Advances in Well Test Analysis, Monograph Series, *Soc. Pet. Eng.*, Dallas, Texas, 1978, 5.

Eaton Operating Company, Inc., 1990, *Final Contract Report*, prepared for the U.S. Department of Energy under Contract No. DE-AC07-85ID12578, 1990.

Ewing, T. E., M. P. R. Light, and N. Tyler, 1984, "Integrated Geologic Study of the Pleasant Bayou-Chocolate Bayou Area, Brazoria County, Texas - First Report," *Consolidation of Geologic Studies of Geopressured Geothermal Resources in Texas: The University of Texas at Austin, Bureau of Economic Geology, Section IV*, report prepared for Department of Energy, Division of Geothermal Energy, Contract No. DE-AC08-79ET27111, 1984, pp. 90-142.

Fahrenthold, E. P., and K. E. Gray, 1985, "Compaction of Geopressured-Geothermal Reservoir Rock," *Proceedings, Sixth Geopressured Geothermal Energy Conference*, The University of Texas at Austin, Center for Energy Studies, M. H. Dorfman and R. A. Morton, eds., 1985, pp. 171-179.

Fowler, W. A., Jr., 1970, "Pressures, Hydrocarbon Accumulation, and Salinities - Chocolate Bayou Field, Brazoria County, Texas," *Journal of Petroleum Technology, 22*, 1970, pp. 411-423.

Hamlin, H. S., and N. Tyler, 1988, "Consolidation of Geologic Studies of Geopressured-Geothermal Resources in Texas," *The University of Texas at Austin, Bureau of Economic Geology*, report prepared for the U.S. Department of Energy, Advanced Technologies Division, Contract No. DE-FC07-85NV10412, 1988.

Hunt, J. M., 1991, "Geopressured Fluid Compartments," unpublished manuscript, prepared for 1991 Geopressured-Geothermal Energy Conference.

Lake, L. W., 1989, *Enhanced Oil Recovery*, Prentice Hall, Englewood Cliffs, New Jersey, 1989.

Loucks, R. G., D. L. Richman, and K. L. Milliken, 1980, "Factors Controlling Porosity and Permeability in Geopressured Frio Sandstone Reservoirs, General Crude Oil/Department of Energy Pleasant Bayou Test Wells, Brazoria County, Texas," *Proceedings, Fourth Geopressured Geothermal Energy Conference*, The University of Texas at Austin, Center for Energy Studies, M. H. Dorfman and W. L. Fisher, eds., 1980, pp. 46-84.

Mathews and Russel, 1978, "Pressure Buildup and Flow Tests in Wells," *Soc. Pet. Eng.*, Dallas, Texas, 1978, 1.

McCain, W. D., Jr., 1973, *The Properties of Petroleum Fluids*, PennWell Books, Tulsa, OK, 1973, pp. 279-281.

Morton, R. A., T. E. Ewing, and N. Tyler, 1983, "Continuity and Internal Properties of Gulf Coast Sandstones and Their Implications for Geopressured Fluid Production," *The University of Texas at Austin, Bureau of Economic Geology Report of Investigations, 132*, 1983.

Negus-de Wys, J., 1992, *The Geopressured Habitat, A Selected Literature Review*, EGG-EP-9982, September 1992.

Osif, T. L., 1984, "The Effects of Salt, Gas, Temperature, and Pressure on the Compressibility of Water," SPE 13174, *59th Annual Technical Conference and Exhibition of the SPE*, Houston, Texas, September 16-19, 1984.

Ostermann, R. D., A. Bloori, and K. Dehghani, 1985, "The Effect of Dissolved Gas on Reservoir Brine Viscosity," SPE 14211, *60th Annual Technical Conference and Exhibition of the SPE*, Las Vegas, NV, September 22-25, 1985.

Powley, D. E., 1987, "Subsurface Fluid Compartments," *Gas Research Institute Deep Gas Sands Workshop*, Chicago, 1987.

Perry's Chemical Engineers' Handbook, Fourth Edition, 1963, R. Perry, C. Chilton, and S. Kirkpatrick, eds., McGraw-Hill Book Co., 1963, pp. 3-199 and 3-200.

Price, L. C., C. W. Blount, D. MacGowan, and L. Wenger, 1981, "Methane Solubility in Brines with Application to the Geopressured Resource," *Proceedings, Fifth Conference on Geopressured-Geothermal Energy*, Louisiana State University, October 1981, pp. 205-214.

Rodgers, J. A., 1982, Drilling and Completion of Pleasant Bayou No. 2, Brazoria County, Texas, Final Report, Volume 2," Submitted to Fenix & Scisson, Inc., by Gruy Federal, Inc., under Contract No. SC-PB-80-374, December 31, 1982.

Saad, N., 1989, *Field Scale Simulation of Chemical Flooding*, Ph.D. dissertation, University of Texas, Austin, August 1989, p. 51.

Shook, M., and D. D. Faulder, 1991, *Validation of a Geothermal Reservoir Simulator*, EGG-EP-9851, October 1991.

Stevens, J. E., and J. D. Clark, 1980, "Completion and Testing of No. 2 Pleasant Bayou Well," *Proceedings, Fourth Geopressured Geothermal Energy Conference*, University of Texas at Austin, Center for Energy Studies, M. H. Dorfman and W. L. Fisher, eds., 1980, pp. 200-210.

Tomson, M. B., J. M. Matty, and L. R. Durrett, 1985, "Saturation Index Predicts Brines Scale-Forming Tendency," *Oil and Gas Journal,* March 1985.

Tyler, N., and J. H. Han, 1982, "Elements of High Constructive Deltaic Sedimentation, Lower Frio Formation, Brazoria County, Texas," *Trans., Gulf Coast Association of Geological Societies, 32*, 1982, pp. 527-540.

Vinsome, P. K. W., 1990, *TETRAD Users Manual*, Dyad Engineering, Calgary, Alberta, Canada, 1990.

Vinsome, P. K. W., and G. M. Shook, 1992, "Multipurpose Simulation," to appear, *Journal of Petroleum Engineering and Engineering*, 1992.

Appendix A.   Transient Test Analyses

Many different types of transient tests are used to obtain reservoir and well data. Only techniques that have been used to analyze Pleasant Bayou reservoir are discussed in this appendix. Derivations of the working equations are omitted, but the derivations are available in standard references (e.g., Earlougher, 1976).

A total of six periods in the history of the Pleasant Bayou #2 (PB2) well are amenable to transient test analysis. These periods include the four "conventional" transient tests, in which bottomhole pressure measurements were made. Other periods also exist when well operations were conducive to transient test analysis. Conventional transient tests that have been conducted are:

1. September 15, 1980 -   Reservoir Limits Test
        December 15, 1980   (drawdown and buildup)

2. May 26, 1988 - June 1, 1988   Multirate Test
                                   (drawdown and buildup)

3. May 15 - 18, 1989   65-Hour Buildup Test

4. April 28, 1992 - June 1, 1992 Constant Rate Test
                                   (drawdown and buildup)

While these transient tests have been useful in establishing near-well reservoir properties (e.g., permeability, fault locations) and well effects (skin), other reservoir properties such as volume and shape cannot be determined from these tests. Fortunately, there have been two times in which well production rate was kept constant for long periods. When a well is produced at a constant rate for a sufficient period, the reservoir enters what is known as pseudo-steady state. In this case, the pressure everywhere in the reservoir declines at a constant rate with time. From an analysis of these data, one is able to estimate such reservoir parameters as drainage volume and shape. After each of these periods of constant production rate, the well was shut in for extended times, thus allowing an estimation of average reservoir pressure. Therefore, despite an absence of downhole pressure measurements at these times, analysis of the pressure transients can provide good approximations to these critical reservoir properties. The periods that have been analyzed are as follows:

1. October 1989 - July 1990   5,100+ hours of constant rate
                                      followed by 1,300+ hours of
                                      buildup

2. September 1991 - February 1992   3,500+ hours of constant rate
                                           followed by 1,100+ hours of
                                           buildup

Results from transient analyses are discussed in chronological order in
some detail below.

Transient Analysis Methods

The discussion that follows is not meant to be a detailed treatment of the
theory of transient analysis. Methods discussed are those that have been
used in analyzing transient tests conducted on the Pleasant Bayou
reservoir. No attempt has been made to provide background theory of these
methods; however, detailed derivations of the working equations and
discussions of the techniques can be found in a variety of references
(e.g., Earlougher, 1976; Mathews and Russell, 1967).

When a well is opened to flow in an initially static reservoir, a pressure
transient moves out into the reservoir. Solution of the governing
equations for this case (prior to the pressure transient "seeing" the
reservoir boundaries) gives

$$P_{wf} = m \log(t) + b \qquad (A1)$$

where

$$m = -\frac{162.6 \, q \, B \, \mu}{k \, h}$$

$$b = P_{1hr} = P_I + m\left[\log\left(\frac{k}{\varphi\mu c_t r_w^2}\right) - 3.23 + 0.87S\right]$$

Thus, by plotting the flowing pressure, Pws, vs. log(t) (or vs. t on
semilog paper), a straight line should develop. From Equations (A2) and
(A3), reservoir permeability and well skin can be obtained from the slope,
m, and intercept, b, of the straight line:

$$k = -\frac{162.6 \, q \, B \, \mu}{m \, h} \qquad (A2)$$

$$S = 1.1513\left[\frac{P_I - P_{1hr}}{m} - \log\left(\frac{k}{\varphi\mu c_t r_w^2}\right) + 3.23\right] \qquad (A3)$$

P_{1hr} is the flowing pressure at t = 1 hour, extrapolated from the straight
line.

If, instead of imposing a single rate on the well, multiple (N) rates are imposed, a modification to Equation (A1) is required. By using superposition, it can be shown (Earlougher, 1976) that a plot of

$$\frac{P_i - P_{wf}}{q_N} \text{ vs. } \sum_{i=1}^{N} \frac{q_i - q_{i-1}}{q_N} \log(t - t_{i-1})$$

results in a straight line. Permeability is obtained from the slope of this line:

$$k = -\frac{162.6 \, B \, \mu}{m \, h} \tag{A4}$$

Well skin can also be obtained from this multirate test; however, it is usually more accurate to obtain skin from the single rate Equation (A3), using the first rate of the test.

If a well is flowed for sufficient time, all reservoir boundaries will be "seen" by the pressure transient. At this time, the reservoir enters pseudo-steady state, in which all pressures decline linearly with time. By plotting flowing pressure vs. time, reservoir drainage volume can be estimated from the slope, m, of this line:

$$V_p = -\frac{0.2339qB}{c_t \, m} \tag{A5}$$

If a well is flowing at some rate q for a period t_p, and is shut in for some time Δt, another pressure transient moves into the reservoir. This is known as a pressure buildup test, and, again, reservoir permeability and well skin can be estimated from the pressure response. Superposition of rates (q for t_p + Δt; -q for Δt) allows the shutin pressure Pws to be represented as:

$$P_{ws} = P_i - m \log\left(\frac{t + \Delta t}{\Delta t}\right) \tag{A6}$$

Permeability is again obtained from the slope of the semilog plot:

$$k = -\frac{162.6 \, q \, B \, \mu}{m \, h} \tag{A7}$$

and skin from the intercept:

$$S = 1.1513\left[\frac{P_{1hr} - P_{wf}}{m} - \log\left(\frac{k}{\varphi \mu c_t r_w^2}\right) + 3.23\right] \tag{A8}$$

In this case, P_{1hr} is the shutin pressure at $\Delta t = 1$ hour and P_{wf} is the flowing pressure just prior to shutin. This method is simplified if the reservoir is in pseudo-steady state prior to the buildup test. In this case, a plot of Pws vs. Δt yields a straight line. Permeability is obtained from the slope as in Equation (A7), and skin from Equation (A8).

If the rate has been varied prior to the buildup test, modifications must again be made. If the last rate has been in place long enough so that the reservoir is in pseudo-steady state (pss), effective production time t_p may be estimated from

$$t_p = \frac{Q}{q}$$

Q in this equation is total production since static, equilibrated conditions, and q is the most recent production rate. If, on the other hand, rates have varied significantly and the reservoir is not in pss, superposition must be used to obtain a solution. In this case, a plot of

$$P_{ws} \text{ vs. } \sum_{i=1}^{N} \frac{q_i}{q_N} \log\left(\frac{t_N - t_{i-1} + \Delta t}{t_N - t_i + \Delta t}\right) \tag{A9}$$

yields a straight line. Permeability can be obtained from Equation (A7) with q_N in place of q, and skin is given from Equation (A8).

Among the most important parameters obtained from a pressure buildup test is an estimation of average drainage pressure, P_{avg}. To obtain an estimate of P_{avg}, shutin pressures are extrapolated to infinite shutin time. The extrapolated pressure is known as the false pressure, P*. P_{avg} may then be estimated from P* and from the slope of the pressure buildup plot using Mathews-Brons-Hazebroek (MBH) theory (Earlougher, 1976):

$$P_{avg} = P^* - \frac{m}{2.303} P_{D_{MBH}} \tag{A10}$$

$P_{D_{MBH}}$ plots as functions of reservoir shape are given in a variety of references.

A final analysis tool discussed here concerns a change in the slope of any of the above plots. Wellbore storage effects can cause an apparent increase in the slope, and care must be taken to eliminate data that exhibit storage effects. Another cause of changes in slope arises from the presence of a permeability transition or linear fault. In the case of a permeability transition, and assuming constant compressibility, the ratio of the slopes is inversely proportional to the ratio of permeabilities:

$$\frac{m_1}{m_2} = \frac{k_2}{k_1} \tag{A11}$$

A doubling of the slope may also indicate the presence of a linear fault or flow boundary. From superposition in space, the distance to such a boundary or transition is given by:

$$L_x = 0.01217 \sqrt{\frac{k\, t_{int}}{\phi \mu c_t}} \tag{A12}$$

where t_{int} is the time at which the two straight lines intersect.

Methods discussed above can be used any time well operations change and any time a pressure transient moves into the reservoir. At times, the data obtained from such an analysis can only be used qualitatively; however, such data can and should be used in conjunction with other information and methods of testing. Many times, these qualitative data are helpful in supporting a hypothesis or in suggesting a means of testing a theory. Petrophysical and fluid properties required in these analyses are summarized in Table A1.

Table A1. Reservoir and fluid properties used in transient analyses.

Thickness (middle sand at PB2), h	62 ft
Total compressibility (pore + fluid), c_t	5.96×10^{-6} psi^{-1}
Well radius, r_w	0.29 ft
Fluid viscosity, μ	0.28 cp
Formation volume factor, B_w	1.049 rb/STB
Porosity, ϕ (of middle sand)	0.18

1980 Reservoir Limits Test (RLT)

The 1980 Reservoir Limits Test began September 15, 1980 and consisted of a 45-day drawdown test followed by a 45-day buildup test. Production rates and bottomhole pressures were given by Gruy (Rodgers, 1982). Production rates are given graphically in Figure A1. For purposes of test analysis, these rates have been approximated as:

$$
\begin{array}{llll}
0 \le t \le & 125.5 \text{ hrs} & q = & 6,650 \text{ STB/d} \\
125.5 \le t \le & 360.5 \text{ hrs} & q = & 10,920 \text{ STB/d} \\
360.5 \le t \le & 450.5 \text{ hrs} & q = & 19,160 \text{ STB/d} \\
450.5 \le t \le & 528.5 \text{ hrs} & q = & 15,460 \text{ STB/d} \\
528.5 \le t \le & 859.5 \text{ hrs} & q = & 13,300 \text{ STB/d} \\
859.5 \le t \le & 1,082.2 \text{ hrs} & q = & 13,100 \text{ STB/d}
\end{array}
$$

The first 125 hours of this test can be analyzed using constant rate drawdown theory. Analysis indicates that wellbore storage affects last minutes. The pressure-time plot for the first step of the RLT is given in Figure A2. Slope and intercept taken from this plot are -30.04 psi/cycle and 10,918 psi, respectively. From these data, permeability and well skin are then estimated as 164 md and 0.2.

Figures A3-A4 show the results from each of the rate steps in the RLT. Permeability estimates for these cases, from Equation (A4), range from 160 to 200 md. Given the amount of scatter in production rates during steps 3 and 4, this is considered good agreement.

In examining Figures A3 and A4, one also notes the near doubling of the slopes in steps 5 and 6. As discussed above, a doubling of slopes can indicate the presence of a linear flow barrier or fault; the distance to the fault can be estimated from Equation (A12). The curve for rate step 2 intersects the curve for step 5 at an ordinate value of 1.4, corresponding to a time of approximately 361 hours. Using Equation (A12), the permeability from step 2, and other petrophysical properties as noted in Table 1, the apparent fault is at a distance of 5,900 ft from the test well. This value should be taken as an approximation, however, given the variations in flow rates in the middle of the flow test.

Because of the multiple flow rates used in the drawdown test, the multirate method is used in the buildup analysis. The pressure buildup data are shown in Figure A5. Permeability is estimated from Equation (A4) as 211 md; S = 5, from Equation (A5).

Once again, from Figure A5, we can see an increase in the slope of the line, an indicator of a possible fault. The shutin time at the intersection point is approximately 36 hours; from Equation (A12), we see that the distance to the fault is about 2,100 ft from the test well. The presence of this fault was masked in the drawdown test, possibly due to variations in flow rate. The fact that the slope did not double suggests that this boundary is either not a linear barrier (or is oriented at an oblique angle) or that there is no fault at all, but rather a permeability transition. If it is a permeability transition, distal reservoir permeability can be estimated as 125 md.

Data obtained from the 1980 RLT are summarized in Table A2.

1988 Multirate Test
Upon cleaning out and recompleting the Pleasant Bayou wells in early 1988, EOC conducted a short (92-hour) drawdown test, followed by a 24-hour

buildup. Production rates are given in Figure A6. Rate steps used in the analysis are:

$$0 \leq t \leq 12 \text{ hrs, } q = 4{,}900 \text{ STB/d}$$
$$12 \leq t \leq 24 \text{ hrs, } q = 7{,}400 \text{ STB/d}$$
$$24 \leq t \leq 32 \text{ hrs, } q = 11{,}680 \text{ STB/d}$$
$$32 \leq t \leq 53 \text{ hrs, } q = 11{,}480 \text{ STB/d}$$
$$53 \leq t \leq 58 \text{ hrs, } q = 9{,}500 \text{ STB/d}$$
$$58 \leq t \leq 61 \text{ hrs, } q = 8{,}150 \text{ STB/d}$$
$$61 \leq t \leq 92 \text{ hrs, } q = 9{,}640 \text{ STB/d}$$

Figure A7 shows results of the first step of the drawdown test. Using Equations (A1) and (A2), we find that the permeability is 181 md and well skin is -0.6. Results from the first four rate steps are shown in Figure A8. The values of permeability (150-180 md) obtained from this figure and Equation (A4) again show good agreement with that of the first step and also agree with those found in the 1980 RLT. Due to tool failure, later rate steps were not analyzed. Neither faults (or transition boundaries) detected in the 1980 RLT were detected in this test. The near boundary was possibly missed because of variations in flow rate at early times. The far boundary was not seen because the drawdown test did not last long enough. From Equation (A12), a 92-hour drawdown test could "see" a fault no farther away than 3,100 ft.

The buildup portion of the MRT was analyzed using the multiple rate method described above. Pressure-time data are given in Figure A8. These data suggest a permeability of 162 md and no well skin. Once again, the nearer boundary was not seen, perhaps because of the length of the test. In this case, $L_{xmax} = 1{,}500$ ft from Equation (A12).

Data obtained from the 1988 MRT are also summarized in Table A2.

May 15-18, 1989 Buildup Test
On May 15, 1989, PB2 was shut in for a 65-hour buildup test. Prior to shutin, the production rate was 12,205 STB/d; however, the reservoir had not entered pseudo-steady state because of earlier rate changes. Production time, t_p, was estimated as 12,780 hours from total production May 1988-May 1989 divided by the last production rate.

Buildup results are given in Figure A10. From this figure, permeability is estimated as 193 md and skin is -1.1. Once again, we see an increase in the slope in this figure. From Equation (A12), the distance to this transition is 1,440 ft. This is in reasonably good agreement with the distance found in the 1980 test.

Results from this test are presented in Table A2.

Constant Rate Drawdown, October 1989-May 1990

In October, 1989, a Hybrid Power System (HPS) was installed at Pleasant Bayou. Production rate was held constant during the HPS experiment - approximately 9 months of constant rate. This was not a conventional transient test in the sense that bottomhole pressure was measured; however, a period of constant production this long lends itself nicely to pseudo-steady state analysis. While downhole pressure data are unavailable, P_{BH} correlates well with surface pressures for a given flow rate. Any transients associated with changing flow rates or thermal effects would be attenuated long before pseudo-steady state conditions apply.

Bottomhole pressure from correlations is plotted against time in Figure A11. Prior to the HPS experiment, the well was shut in for 44 days. While this is not sufficient time for reservoir pressures to equilibrate (see below), for the purposes of this calculation, the assumption of static reservoir conditions is adequate. The linear trend of pressure with time from about t = 1,500 hours is obvious. This portion of the drawdown is detailed in Figure A12. The slope from this curve is 0.0256 psi/hr; from Equation (A5), total connected reservoir pore volume is 26.3 billion ft^3. This is approximately 57% of what the UT-BEG terms proximal reservoir volume (Hamlin and Tyler, 1988). It is clear that the total sand volume as reported by Hamlin and Tyler (46.5 billion ft^3) is not currently in pressure communication with the test well.

When the HPS experiment was completed, PB2 was shut in for 57 days, while the HPS was dismantled and the disposal well reworked. One again, while no bottomhole pressure measurements were taken, surface pressures can be used to estimate reservoir properties. Only daily data were reported, so permeability and well skin should be viewed as coarse approximations.

A plot of Pws vs. log(Δt) is given in Figure A13. From this plot, we obtain an estimate for permeability of 196 md. Skin is given as 5.3. In particular, this value of skin is suspect, since no good estimation of flowing pressure P_{wf} at shutin is available. The scarcity of data at early time also precludes "seeing" the near barrier. A near doubling of the slope at late time, however, does occur. From the intersection point (at Δt = 434 hours), this flow boundary is at approximately 7,000 ft.

The long shutin time (57 days) also suggests the possibility of obtaining an estimate of average reservior pressure, P_{avg}. Using the Mathews-Brons-Hazebroek (MBH) method (Mathews, et al., 1954), we estimate a false pressure, P* as:

$$t_p = Q/q = 15,315 \text{ hours}$$

$$P^* = P_{1hr} + m_2 \log(t_p) = 3,960 \text{ psi}$$

The slope of the second straight line is used in the MBH method because of the inferred presence of a barrier (Earlougher, 1976). Effective production time, t_p, is approximated in terms of the last flow rate, q.

The final data required to apply MBH theory is an estimate of the dimensionless production time to pseudo-steady state, $(t_{pD})_{pss}$. From Earlougher (1976), this is

$$(t_{pD})_{pss} = \frac{0.0002637 \; k \; t_{pss}}{\varphi m c_t A}$$

$$= \frac{(0.0002637) \; (180 \; md)(1500 \; hrs)}{(0.18)(0.27 \; cp)(5.96 \times 10^{-6} psi^{-1}(2.63 \times 10^8 ft^2)} = 1$$

In the above equation, average area, A, was taken from the estimate of Vp (2.63×10^{10} ft^3) and from average thickness (100 ft). Using $(t_{pD})_{pss} = 1$, and entering the MBH plots, we find that $(P_D)_{MBH} \approx 1$ for this case. MBH plot selection was based on the figure that entered pss at $(t_{pD}) = 1$. Using $(P_D)_{MBH} = 1$, we can solve for P_{avg}:

$$P_{avg} = P^* - m_2/2.303, \text{ corrected to average depth}$$
$$= 3,910 \; psi + (14,100 \; ft)*(0.4566 \; psi/ft)$$
$$= 10,345 \; psi$$

As a check against MBH P_{avg}, consider a material balance calculation of the mass in place. For a closed system (no recharge):

$$\frac{Q}{V_p} = c_t \; (\; P_I - P_{avg} \;)$$

As of June, 1990, $Q \approx 1.05 \times 10^7$ STB, $c_t = 5.96 \times 10^6$ psi^{-1}, and P_I (at 14,100 ft SS) = 10,718 psi. Then

$$P_{avg} = 10,718 \; psi$$
$$- (61,500,500 \; ft^3)/(5.96 \times 10^{-6} \; psi^{-1} * 26.3 \times 10^{10} \; ft^3)$$
$$= 10,718 - 392$$
$$= 10,326 \; psi.$$

Agreement between these two estimates is excellent. In comparison, after 57 days of pressure buildup, shutin pressure (corrected to depth) is 10,308 psi and is increasing at a rate of 0.06 psi/hr. It would seem, then, that

reservoir pressure will take appreciably longer than 1,500 hours to equilibrate.

Reservoir properties estimated from this test are given in Table A2.

Constant Rate Drawdown, Oct. 1991-Feb. 1992
A second long-term period of constant production rate began in October 1991 and continued until February 1992. In this case, the well was not shut in prior to this drawdown. Figure A14 shows bottomhole pressure vs. time. This ordinate begins at t = 0 only to identify the time required for the reservoir to enter pseudo-steady state from this constant rate (t_p is actually about 19,700 hours at the start of this constant rate test). As can be seen from the figure, psuedo-steady state conditions begin at about t = 1,700 hours. From the slope of the line and Equation (A5), connected reservoir volume is approximately 43.6 billion ft^3, nearly 70% larger than the 1991 volume estimate. Several explanations can be made concerning this apparent drainage volume increase, including increased pore compressibility, a free gas saturation, and influx from an adjacent sand. We exclude the possibility of a gas cap, as the brine is undersaturated with respect to gas. The other two possible explanations are discussed in more detail below.

Perhaps a more conservative way of looking at the pseudo-steady state calculations for reservoir volume is to note that the product (reservoir volume · total compressibility) has increased by a factor of 66% between the two tests. This is seen by solving Equation (A5) for $V_p c_t$. Three possible explanations exist for this increase in the product: either one of the two factors increased by 66%, or both increased by some smaller amount such that the product increased by 66%. Farenthold and Gray (1985) suggest that a representative value of pore compressibility is 3-6 x 10^{-7} psi^{-1}. The value used here is the mean of this range, 4.5 x 10^{-7} psi^{-1}. Using the largest value given by Farenthold and Gray, maximun total compressibility (pore and brine) is 7.07 x 10^{-6} psi^{-1}, an increase of only 18%. This suggests that the minimum pore volume multiplier is 1.66/1.18, or 1.42. Clearly, some recharge from an adjacent aquifer must be taking place.

It is worth noting that it is the product of reservoir volume and total compressibility that actually drives recovery from the geopressured compartment. Furthermore, the individual factors do appear in such a manner as to separate their effects. From this point of view, it matters little whether the reservoir volume has changed or the pore compressibility has changed. However, changes in pore compressibility would likely first be seen at the production well, where changes in effective stress are greatest. Thus far, no obvious change has been observed. Given these observations and the estimated maximum changes from above, we hypothesize

that the total compressibility has remained constant; and the drainage volume has increased by 66%. In the absence of additional data or evidence of changes in compaction, this appears to be a reasonable selection.

Results from this analysis are summarized in Table A2.

47-Day Buildup

After producing at a constant rate for more than four months, production rates were reduced due to surface equipment problems. Production rates are given below:

$$
\begin{array}{llll}
\text{September 26, 1991} & \text{- February 10, 1992} & q = 23,176 \text{ STB/d} \\
\text{February 10, 1992} & \text{- February 12, 1992} & q = 15,387 \text{ STB/d} \\
\text{February 12, 1992} & \text{- February 17, 1992} & q = 22,303 \text{ STB/d} \\
\text{February 17, 1992} & \text{- March 12, 1992} & q = 11,949 \text{ STB/d}
\end{array}
$$

On March 13, the well was shut in for equipment repairs; it remained shut in for 47 days.

This pressure buildup test was analyzed using the multi-rate buildup approach. Pws vs. the reduced time variable from Equation (A9) is plotted in Figure A15. Once again, given the scarcity of early time data, skin and permeability should be treated as qualitative information only. From the Equations (A6) and (A7), we obtain estimates for permeability of 153 md, and S = -0.5. Also from Figure A15, a second linear portion develops, intersecting the original line at t = 494 hours. Using Equation (A12) and the value for permeability obtained above, we estimate the distance to this fault as 6,700 ft. This is again in good agreement with previous estimates.

The length of the buildup test once again suggests the possibility of estimating average reservoir pressure. Following the same procedure as above, the false pressure P* is estimated as 3,870 psi. Using the new values for permeability, average area, and time to pseudo-steady state, we estimate $(t_{pD})_{pss}$ as:

$$
(t_{pD})_{pss} = \frac{0.0002637 \, k \, t_{pss}}{\varphi \mu c_t A} = 0.6
$$

Entering the MBH plots again, P_{DMBH} is again approximately 1; then

$$
\begin{aligned}
P_{avg} &= P^* - m_2/2.303, \text{ corrected to average depth} \\
&= 3,805 \text{ psi} + (14,100 \text{ ft})*(0.4566 \text{ psi/ft}) \\
&= 10,243 \text{ psi}
\end{aligned}
$$

As a check, we once again consider the material balance equation, solving for P_{avg}:

$$P_{avg} = 10,718 \text{ psi}$$
$$-(132,700,000 \text{ ft}^3)/(5.96 \times 10^{-6} \text{ psi}^{-1} * 43.6 \times 10^{10} \text{ ft}^3)$$
$$= 10,718 - 510$$
$$= 10,207 \text{ psi}.$$

As before, agreement between these two estimates of P_{avg} is good. In contrast to these estimates, at day 47 of the pressure buildup test, Pws = 9,980 psi and is increasing at a rate of 0.08 psi/hr.

Results of the analysis are also summarized in Table A2

April 1992 Transient Tests
Upon fixing the surface equipment problems, short-term drawdown and buildup tests were conducted, beginning April 28, 1992. The well flowed 25 hours at a constant rate of 11,215 STB/d. However, due to downhole tool failure, only the first 3 hours of drawdown are available.

The drawdown test is plotted in Figure A16. A straight line develops shortly before tool failure; from Equation (A2), the permeability is 199 md. Using Equation (A3) and P_{1hr}, well skin is estimated to be -1.8. However, the initial pressure used in this analysis is not equal to the static reservoir pressure. From Equation (A3), this would underestimate skin. Using the average reservoir pressure of 10,240 psi, as estimated from MDH theory above, skin is found to be -0.2. The true value of skin is probably between 0 and -2.

Pressure buildup data are plotted in Figure A17. From this figure and Equations (A7) and (A8), permeability is 190 md, and skin is -2. This value of skin is also sensitive to the nonstatic reservoir conditions at the onset of the test and probably represents a lower bound. Finally, a doubling of the slope again suggests the presence of a permeability transition or boundary. The lines intersect at 14 hours; from Equation (A12), the inferred boundary is at about 1,260 ft.

Test results are summarized in Table A2.

Summary of Test Results
Eleven pressure transients have been analyzed for reservoir and well information. Most of the data give very good agreement. For example, reservoir permeability appears to be about 180 md (average values of test results). Well skin, with one notable exception is ~0 - -2. The only case in which the skin was appreciably different from 0 was the 1980 RLT buildup

test (the value of 5.3 from the 57-day buildup is highly suspect and is neglected). No explanation is available for this anomalous value. For purposes of simulation, we use S = 0.

Two distinct faults or permeability barriers were observed from a number of the tests. The closest to the well is located at about 1,600 ft from the well. Based on the slope increases (less than 2 in all but one case), this is inferred to be either a fault oriented at an oblique angle relative to the flow, or a permeability transition. If indeed it is a transition, distal reservoir permeability is approximately 110-120 md. The second fault lies approximately 6,500 ft from PB2.

Reservoir volume calculations are clearly the most controversial of the results presented here. The onset and behavior of pseudo-steady state in both of the long-term constant rate flow tests clearly show that reservoir conditions have changed between test dates. Given the lack of evidence of reservoir failure near the wellbore (where effective stresses are greatest), a large fluid volume increase is inferred. At this point, there is no clear-cut way to determine the manner of this recharge mechanism. Pressure continuity with an adjacent aquifer, episodic flow of brine through a seal, and one-time influx of fluids would all give the same pressure response at the test well.

Table A2. Summary of transient test analyses for Pleasant Bayou Reservoir.

Test	Test Duration	Perm (mD)	Skin	Reservoir Volume	Faults/ Barriers	Average Reservoir Pressure	Comments
RLT - 1980 Drawdown	1,080 hrs	160-200	0.2		5,900 ft.		Fault location questionable, based on steps 2,5. Data good early only.
RLT - 1980 Buildup	1,080 hrs	211	5.		2,100 ft		$m_2 = 1.67\ m_1$; $k_2 = 125$ mD Data quality good.
MRT - 1988 Drawdown	50 hrs w/ tool	150-180	-0.6		none		Good agreement in perms /step. No long data - tool failed. Data good from Steps 1-4.
MRT - 1988 Buildup	24 hrs	162	0.		none		24 hr buildup; Data quality good.
May 89 Buildup	65 hrs	193	-1.1		1,440		$m_2 = 1.7\ m_1$; $k_2 = 115$ Data quality good.
Const. Q - Oct 89-May 90 Drawdown	5,000+ hrs			2.63×10^{10} ft^3			Well shut-in 44 days before test. No bottom hole measurements. Good indicator of pss.
57-Day Buildup June-July 90	1,360+ hrs	196	5.3		7,100 ft.	fr Material Balance: 10326 psi fr. MBH Theory: 10345 psi after shutin Pws = 10308 and increasing 0.06 psi/hr	No tool in hole; skin suspect (no good Pwf). Data good for P_{avg}, not for k,S.
Const Q - Oct 91 - Mar 92	3,280+ hrs			4.36×10^{10} ft^3			No shut-in prior to flow; No bottomhole measurements
47 Day Shutin Mar-Apr 92	1,125+ hrs	153	-0.5		6,700 ft.	fr Material Balance: 10207 psi fr MBH Theory: 10243 psi after shutin Pws = 9980 and increasing 0.08 psi/hr	No bottomhole measurements. Data good for P_{avg}, not for k,S.
Apr 28, 1992 Tests Drawdown	3 hrs	199	-1.8				Only 3 hrs Pwf; $P_I \neq P_{avg}$, so skin suspect.
Apr 28, 1992 Tests Buildup	58 hrs	190	-2.		1,260 ft.		$m_2 = 2.2\ m_1$; $k_2 = 90$ mD. S suspect ($P_I \neq P_{avg}$)

Figure A1. Production Rate for 1980 RLT.
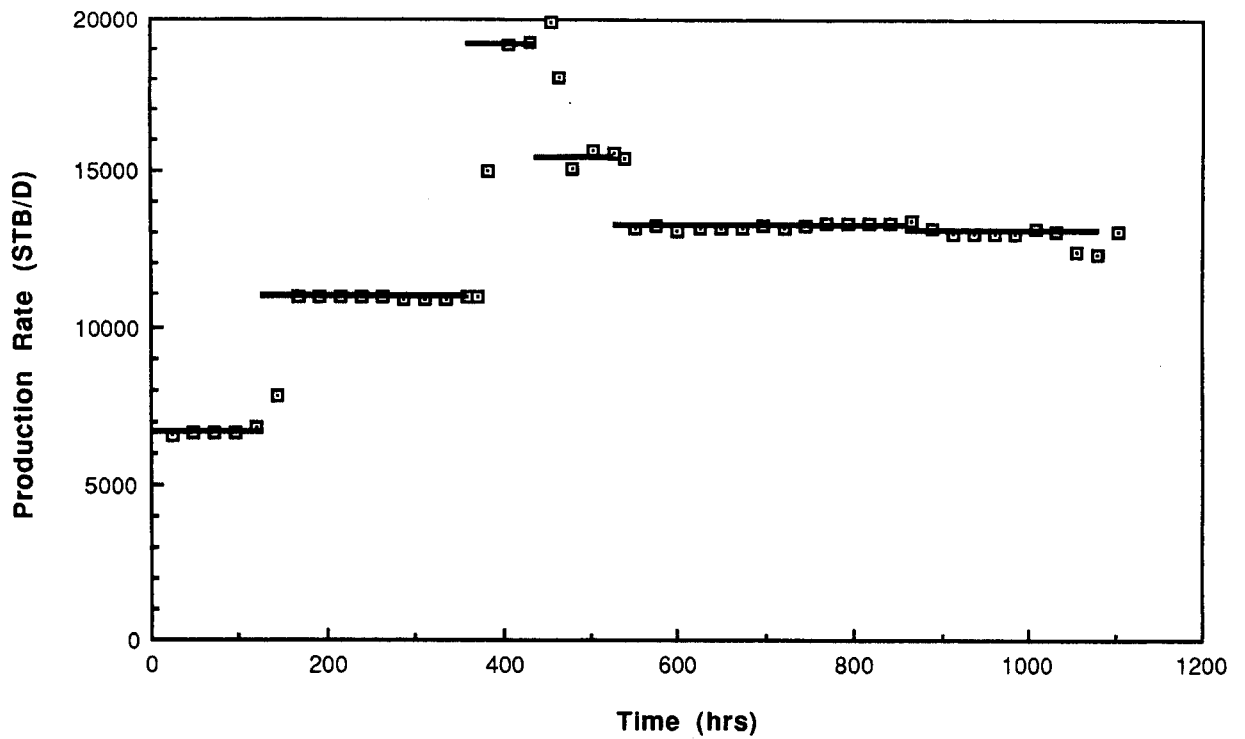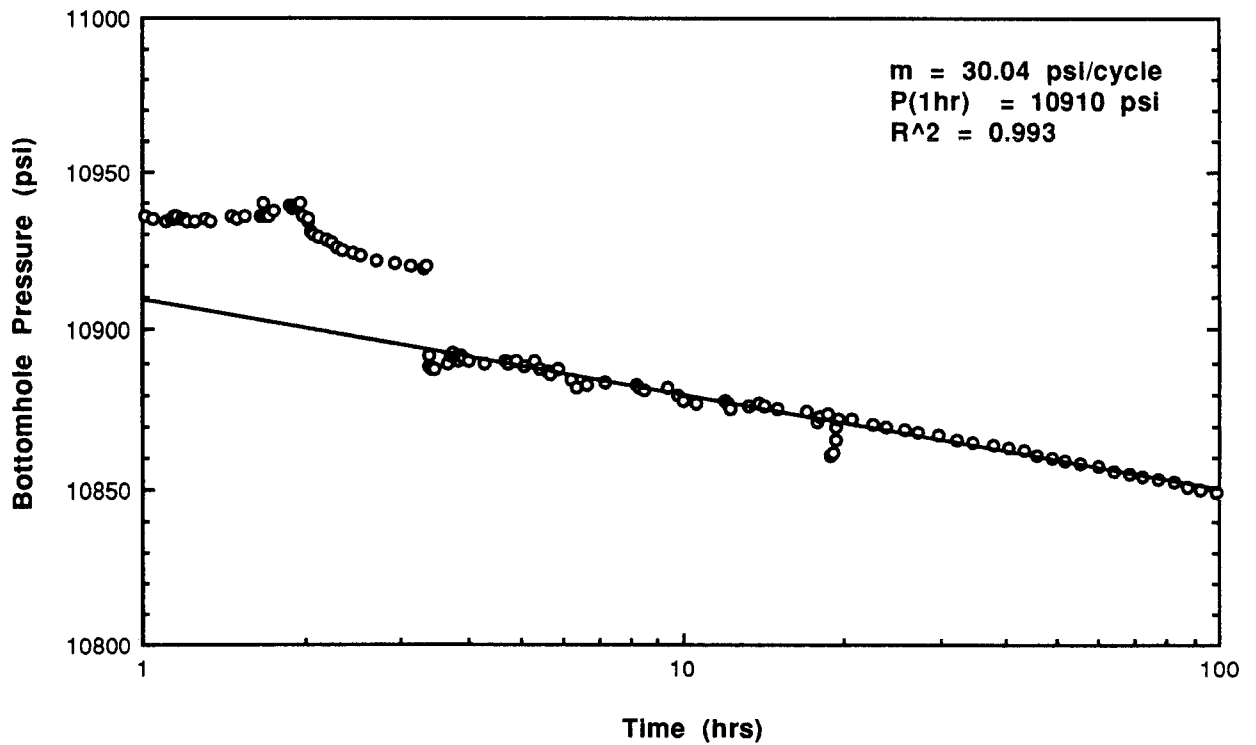

Figure A2. Step 1 of 1980 Reservoir Limits Test.

m = 30.04 psi/cycle
P(1hr) = 10910 psi
R^2 = 0.993

Figure A3. Steps 1-3 of 1980 RLT.

m1 = 0.0051 psi/STB/D
m2 = 0.0053 psi/STB/D
m3 = 0.0045 psi/STB/D

$(PI - Pwf) / q$ (psi/STB/D)

$\{ \Sigma [q_I \log (t - t_{I-1})] \} / q_N$
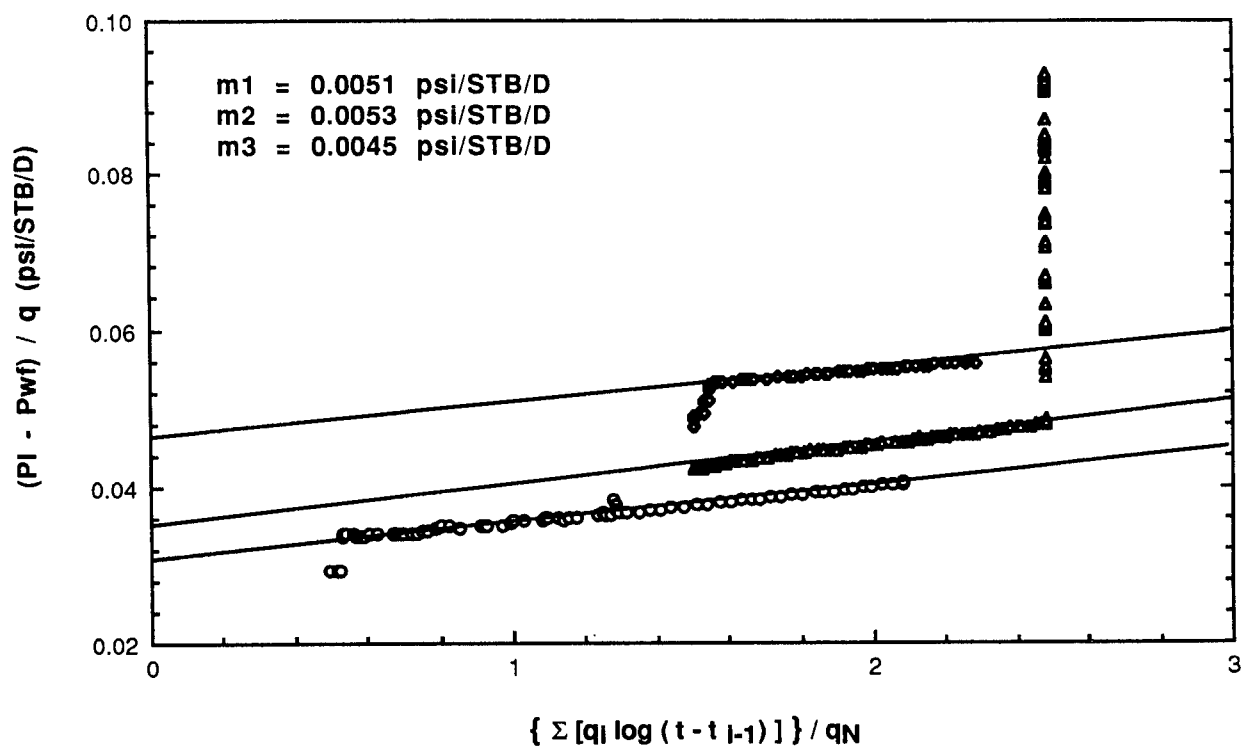
Figure A4. Steps 4-6 of 1980 RLT Test.

m4 = 0.0042 psi/STB/D
m5 = 0.01   psi/STB/D
m6 = 0.013   psi/STB/D

$(Pi - Pwf) / q$ (psi/STB/D)

$\{ \Sigma [q_I \log (t - t_{I-1})] \} / q_N$
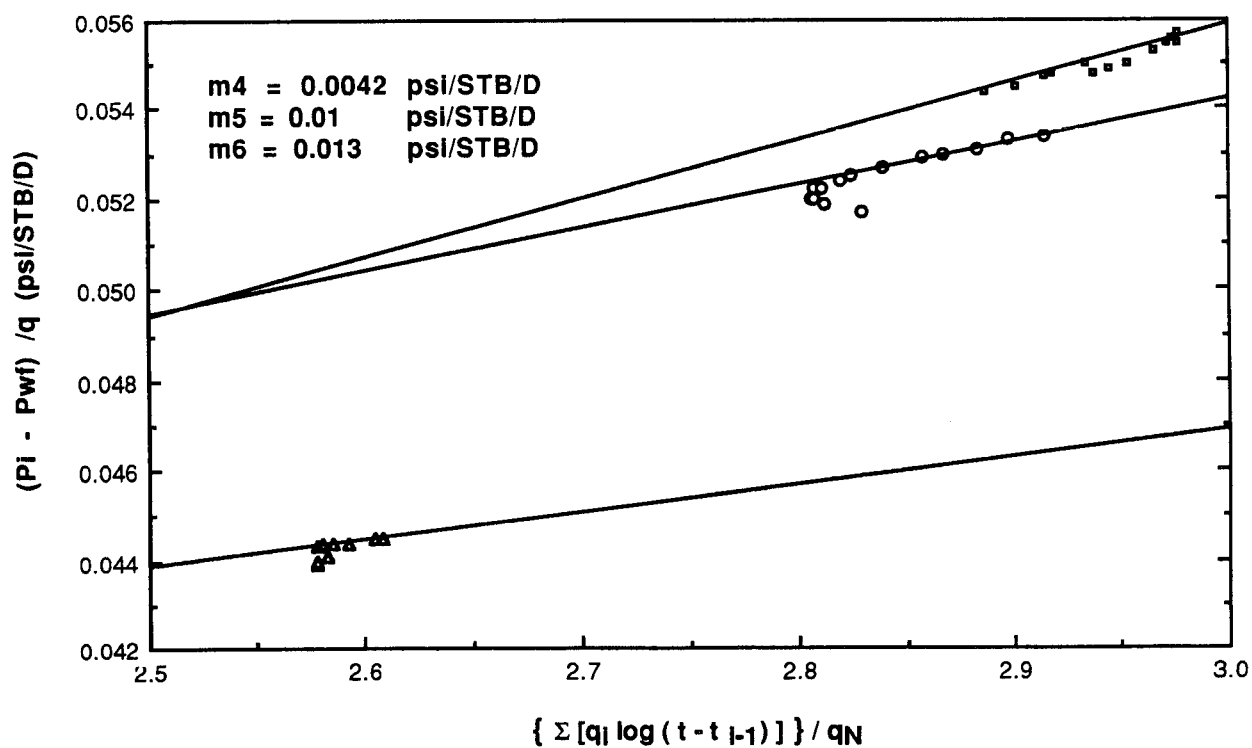
Figure A5. Buildup Portion of 1980 RLT Test.

m1 = 45.85   psi/STB/D
P(1 hr) = 10895 psi

m2 = 76.667 psi/STB/D
t = 36 hrs at intersection

(x-axis) $\Sigma\,(\,q_I\,/\,q_N\,)\,{}^*\,\log\,((\,t\,-\,t_{I-1}\,+\,\Delta t)\,/\,(\,t\,-\,t_I\,+\,\Delta t\,))$

(y-axis) Shut-in Bottomhole Pressure (psi)
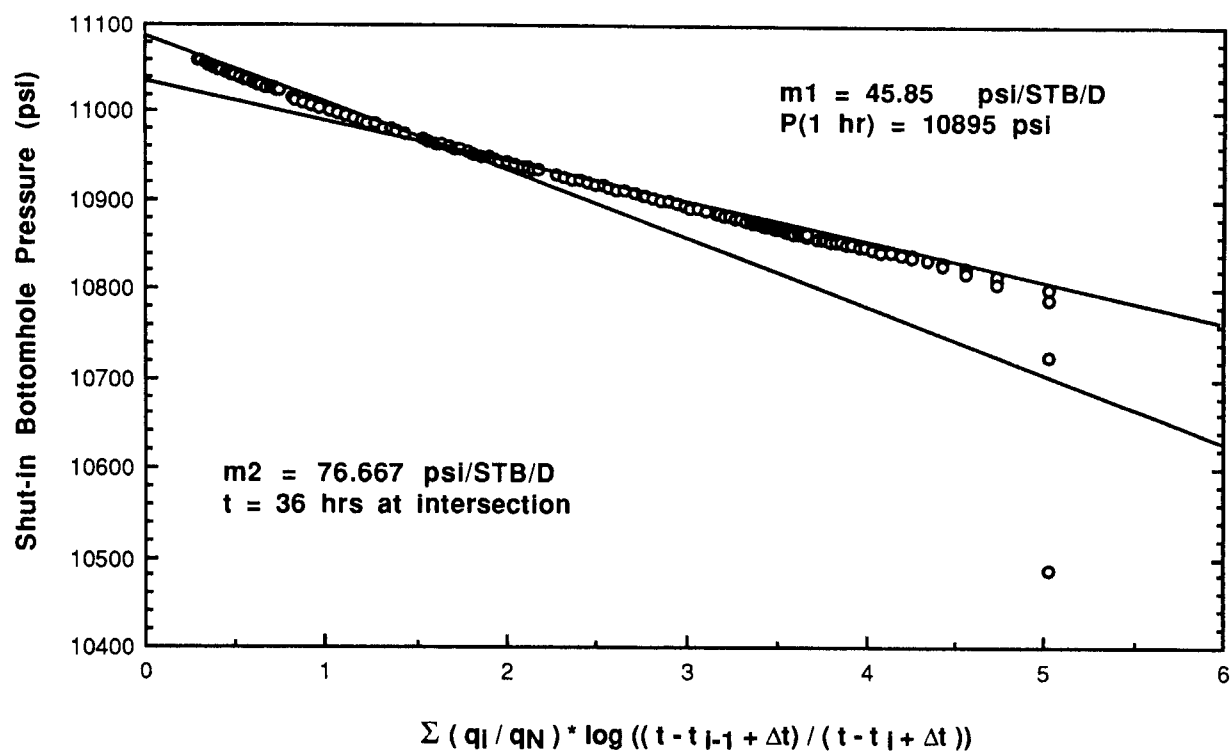
Figure A6. Production Rates for 1988 MRT.

(y-axis) Rate (STB/D)

(x-axis) Time (hours)
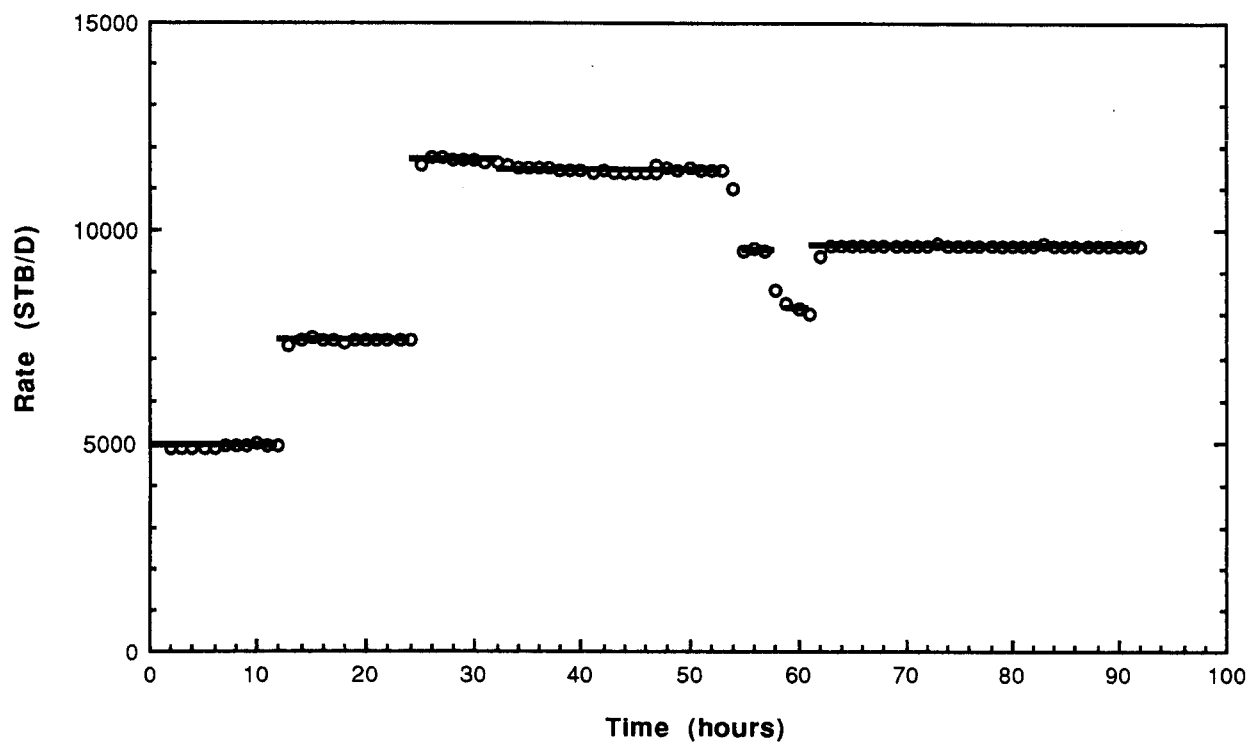
Figure A7. Drawdown Test, Step 1 of 1988 MRT.

m = 20 psi/STB/D
P(1 hr) = 10858 psi

Bottomhole Pressure (psi)

Log (t)
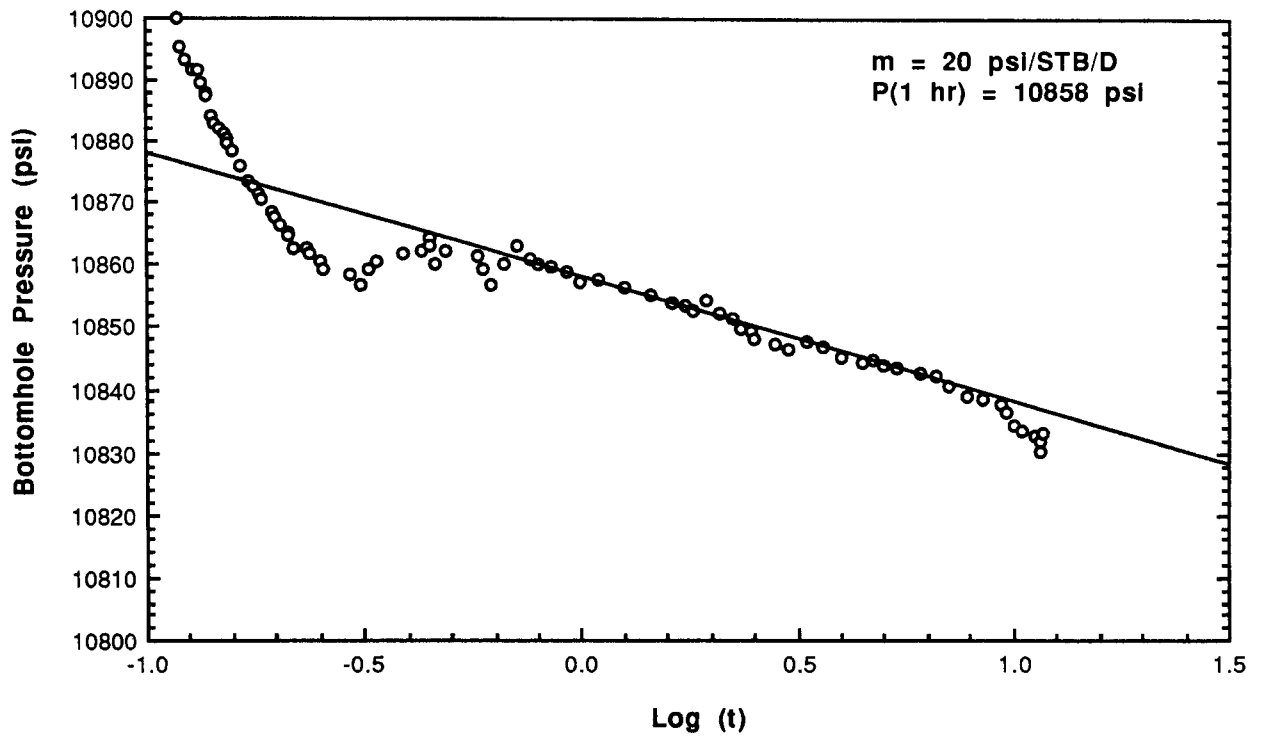
Figure A8. 1988 Multi-Rate Drawdown Test, Steps 1-4.

m1 = -20.4 psi/STB/D

m2 = -23. psi/STB/D

m3 = -23.5 psi/STB/D

m4 = -24 psi/STB/D

Bottomhole Pressure (psi)

$\{ \Sigma [q_i \log (t - t_{i-1})] \} / q_N$
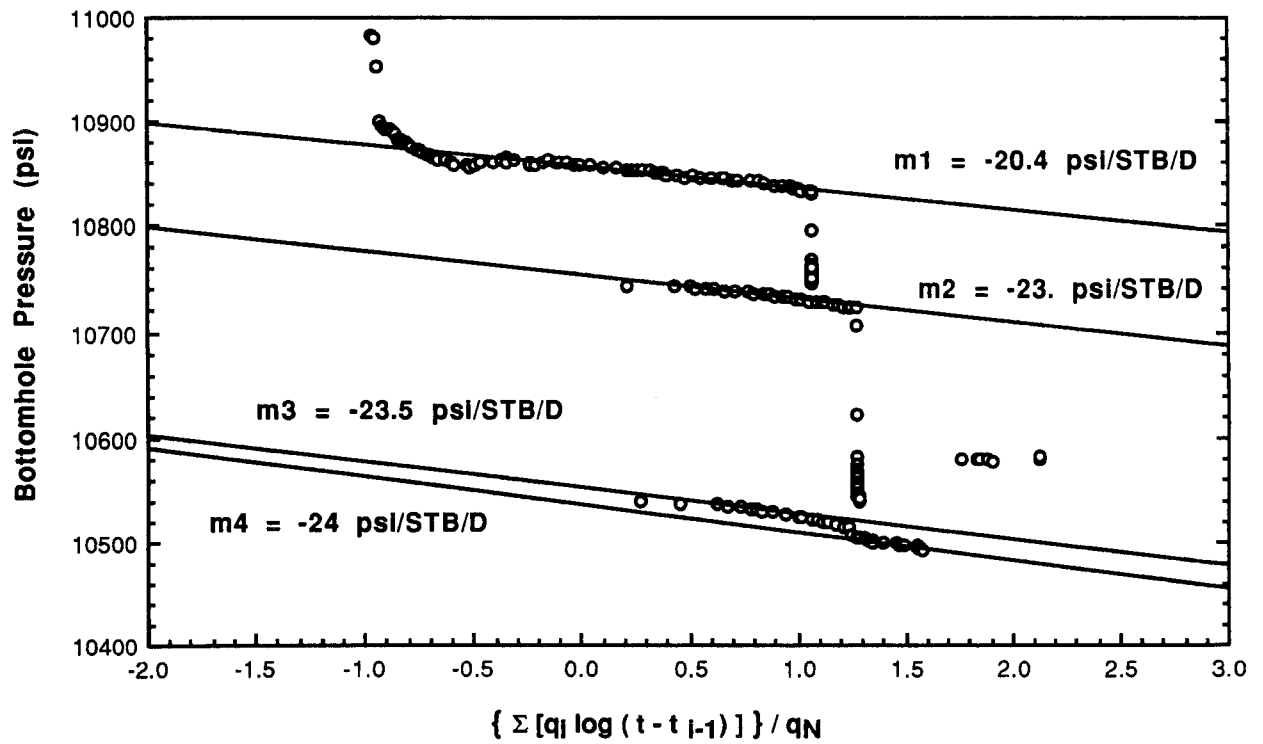
Figure A9. 1988 MRT Buildup Test.

m = 44 psi/STB/D
P(1 hr) = 10871 psi
Pws = 10577 psi

$$\Sigma\,(\,q_I\,/\,q_N\,) * \log\{\,(\,t - t_{I-1} + \Delta t)\,/\,(\,t - t_I + \Delta t\,)\,\}$$
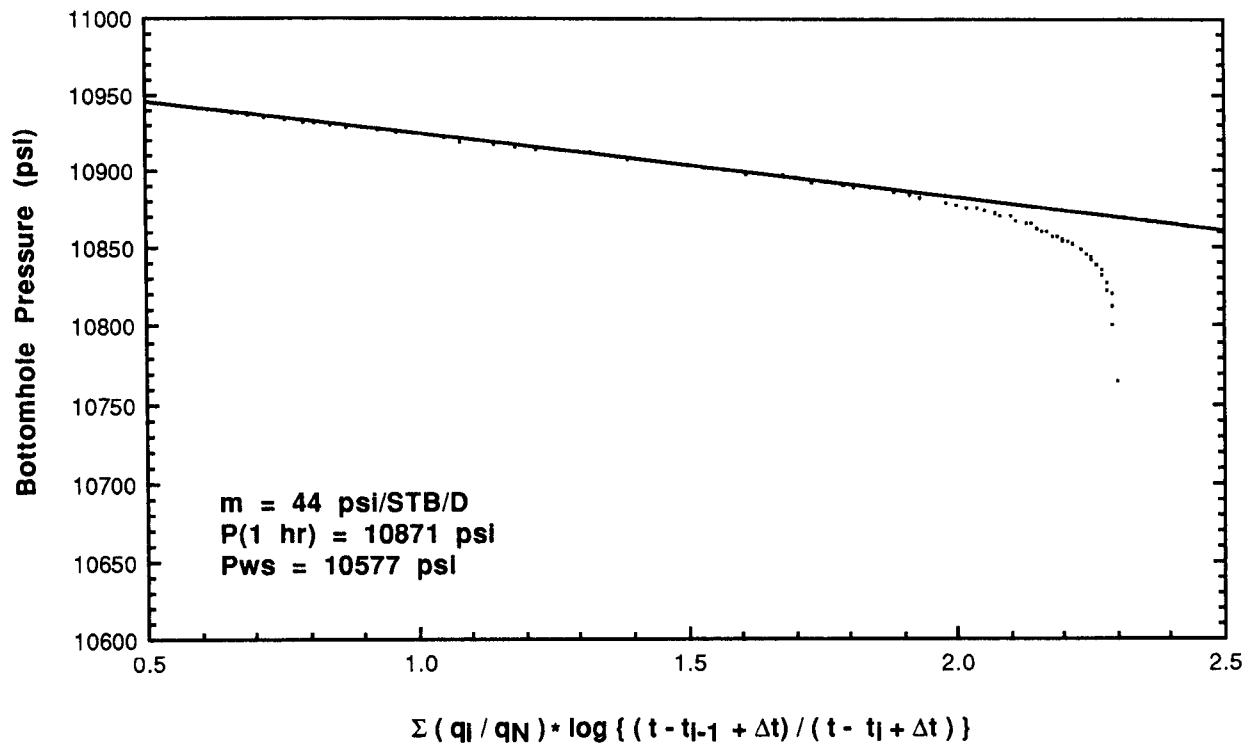
Figure A10. Pressure Buildup Test, May 15-18, 1989.
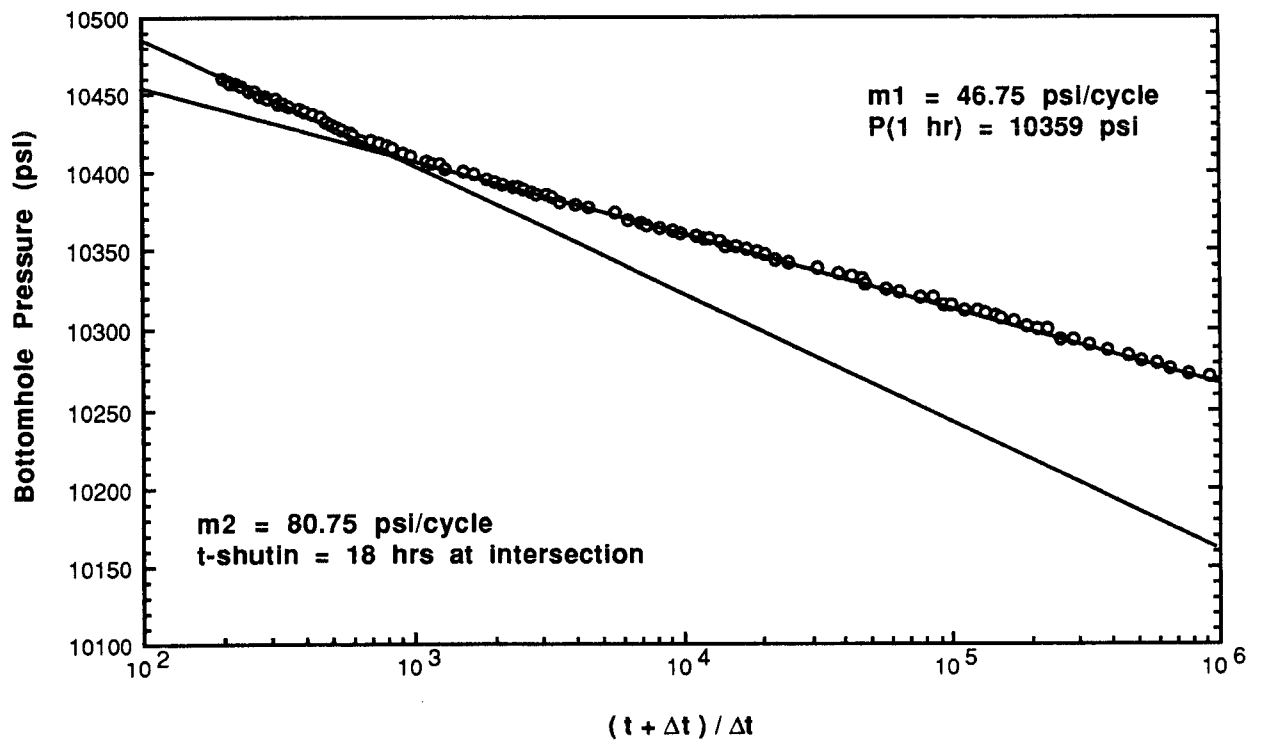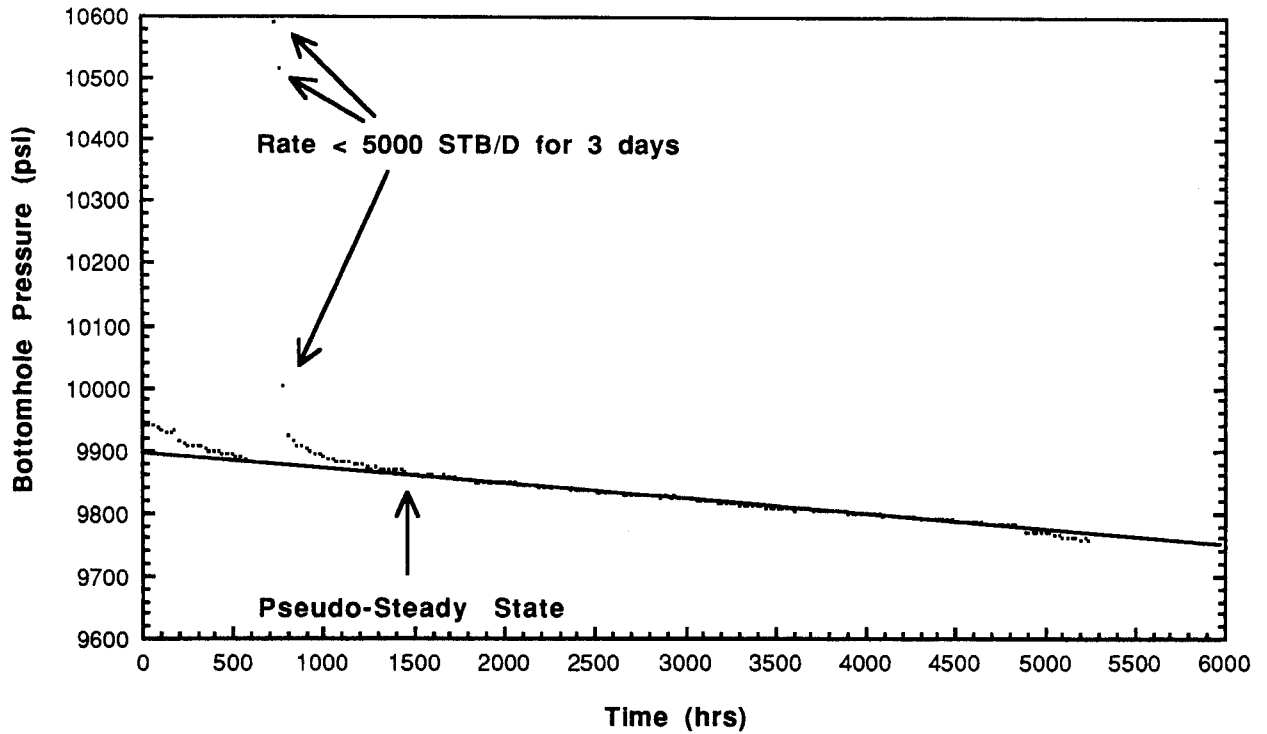
m1 = 46.75 psi/cycle
P(1 hr) = 10359 psi

m2 = 80.75 psi/cycle
t-shutin = 18 hrs at intersection

$$(\,t + \Delta t\,) / \Delta t$$

Figure A11. Bottomhole Pressure History
Oct 24, 1989 — May 31, 1990

Figure A11. Bottomhole Pressure History Oct 24, 1989 — May 31, 1990

Figure A12. Pseudo-Steady State Portion of Constant Rate
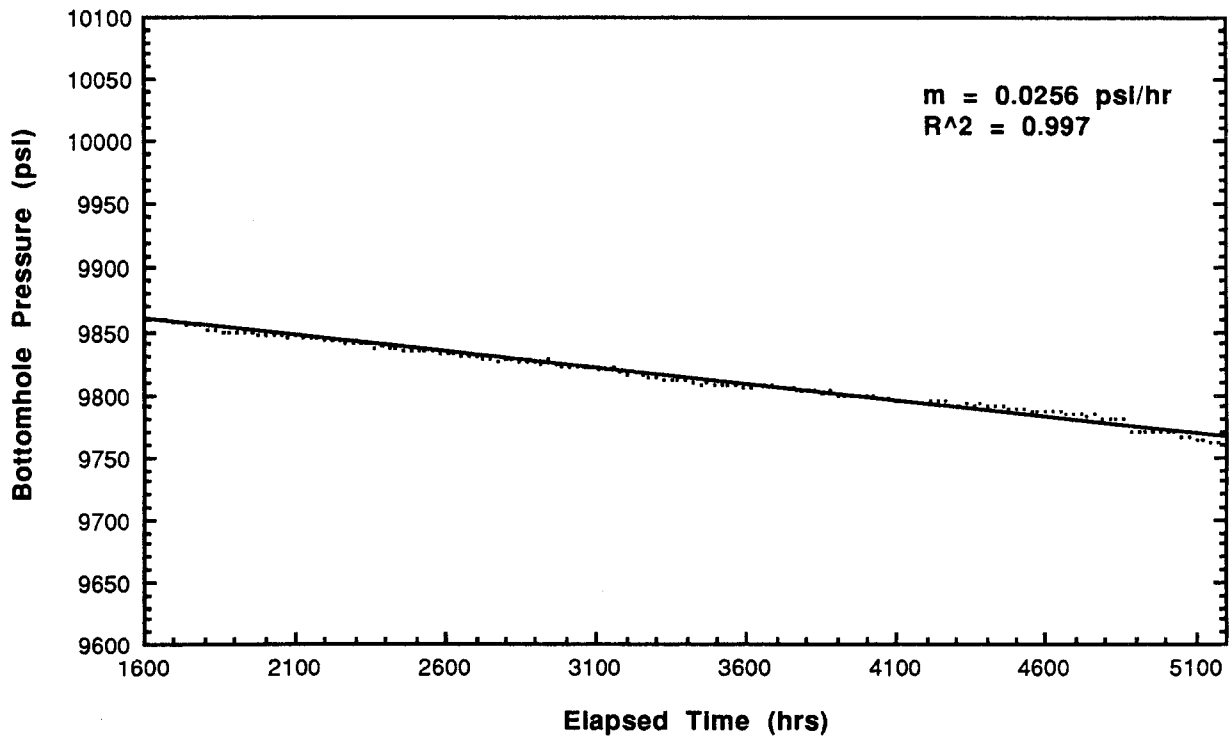## Drawdown Test — Oct 1989 - May 1990.

Figure A12. Pseudo-Steady State Portion of Constant Rate Drawdown Test — Oct 1989 - May 1990.

Figure A13. June-July 1990 Pressure Buildup Test.
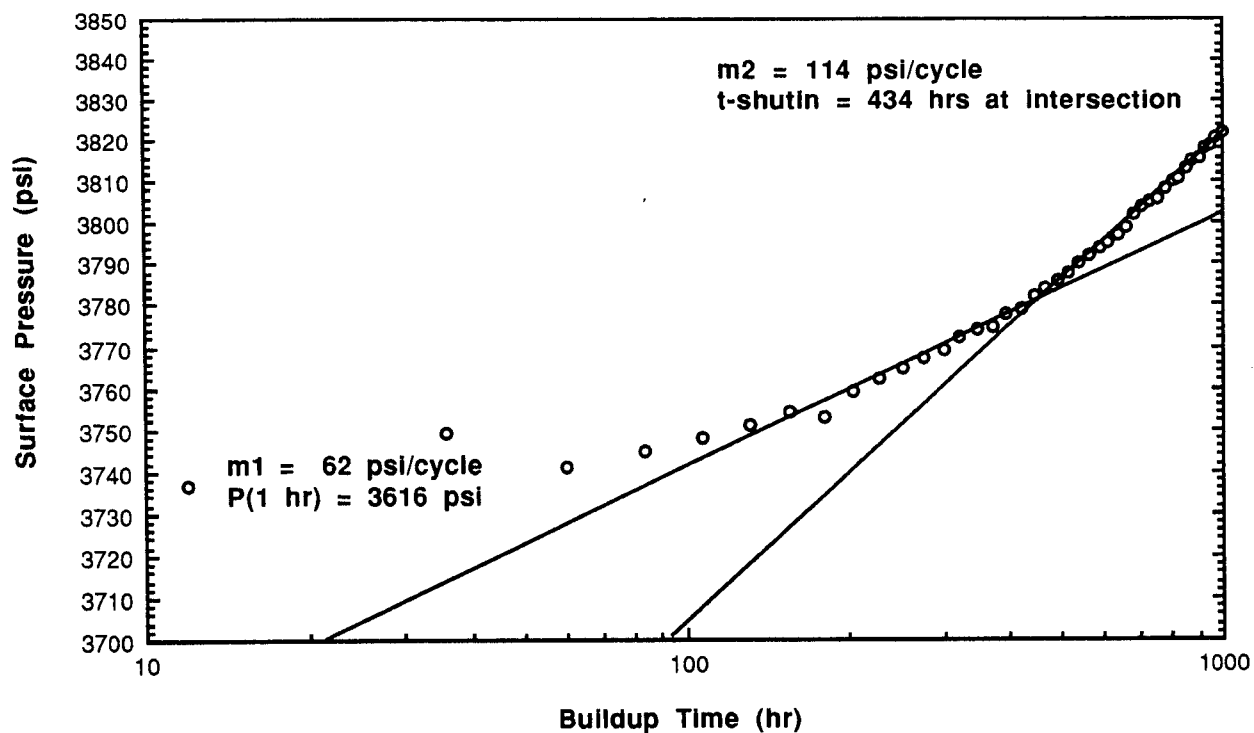

m2 = 114 psi/cycle
t-shutin = 434 hrs at intersection

m1 = 62 psi/cycle
P(1 hr) = 3616 psi

Surface Pressure (psi) — Buildup Time (hr)

Figure A14. Sept. 1991 — Feb 1992 Constant Rate Drawdown Test.

m = 0.0218 psi/hr
R^2 = 0.91

Onset of PSS

Bottomhole Pressure (psia) — Time (hrs)
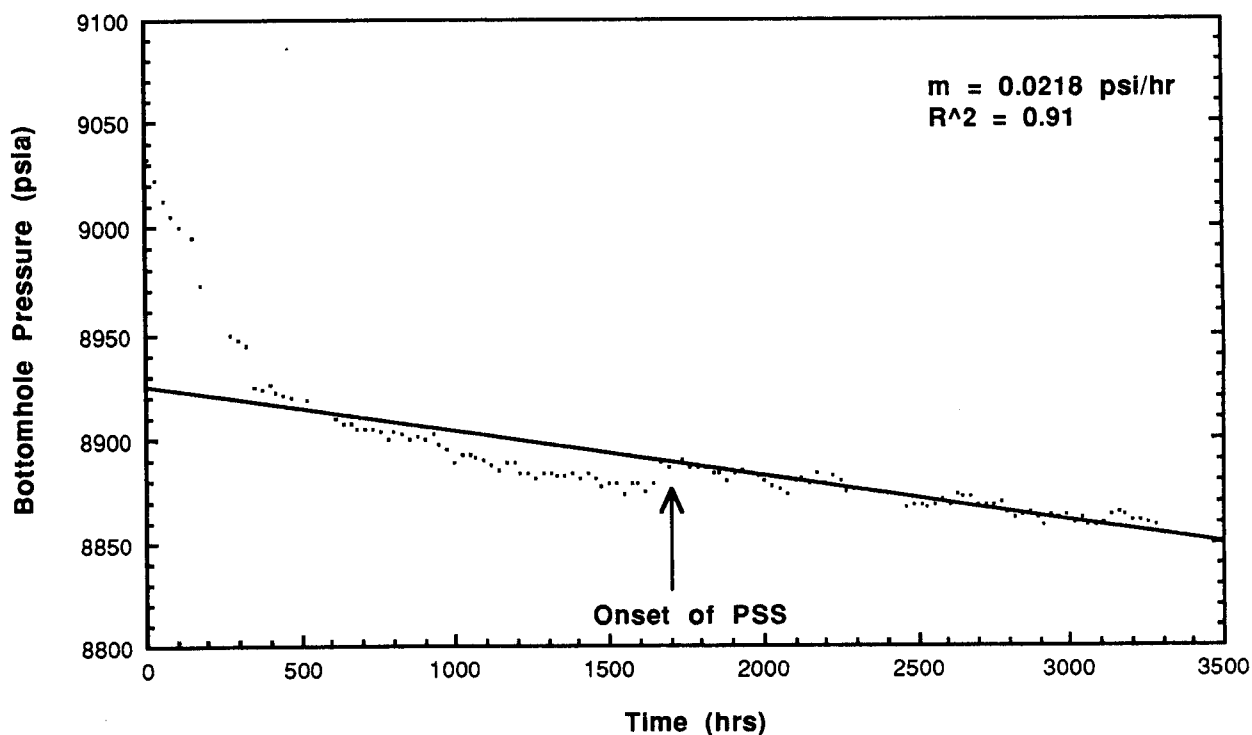
Figure A15. March - April 1992 Buildup Test.

m2 = 150 psi/STB/D
t-shutin = 492 hrs at intersection

m1 = 58.3 psi/STB/D
P(1 hr) = 3261 psi

$\Sigma (q_N / q_i) \log \{(t - t_{i-1} + \Delta t)/(t - t_i + \Delta t)\}$
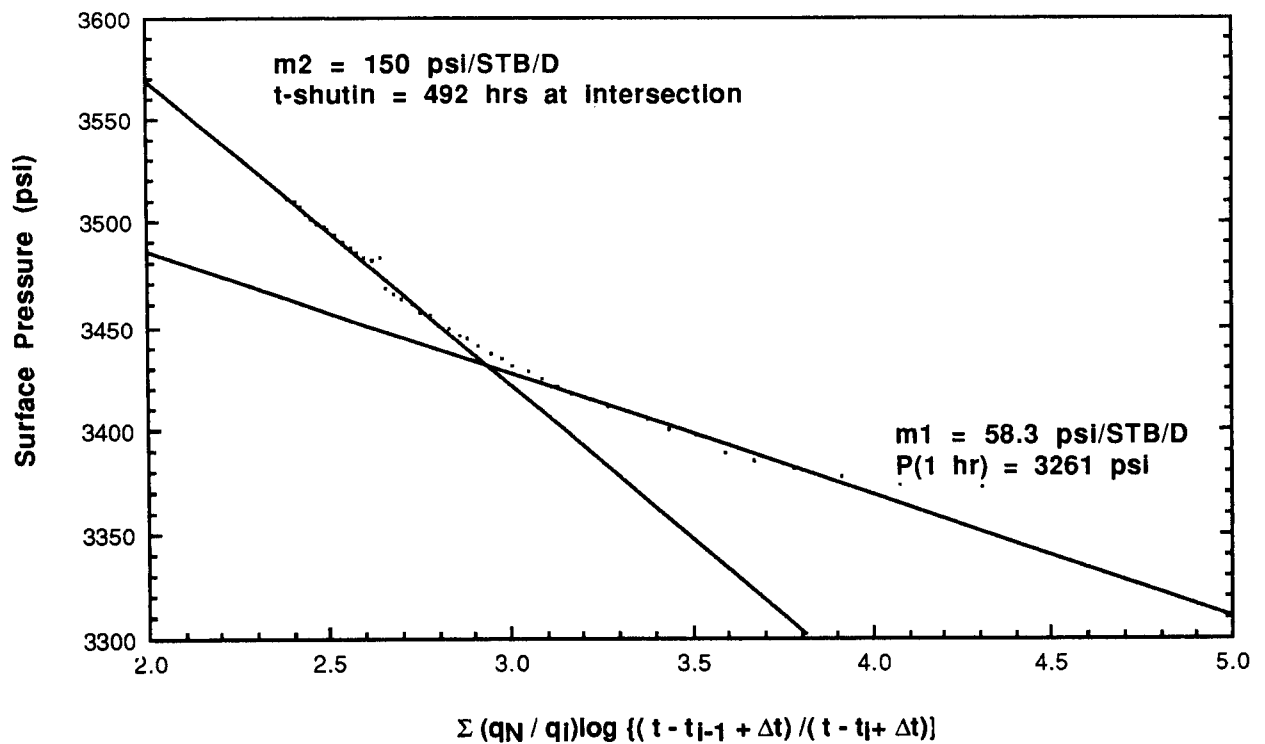
Figure A16. Apr. 28, 1992 Drawdown Test.
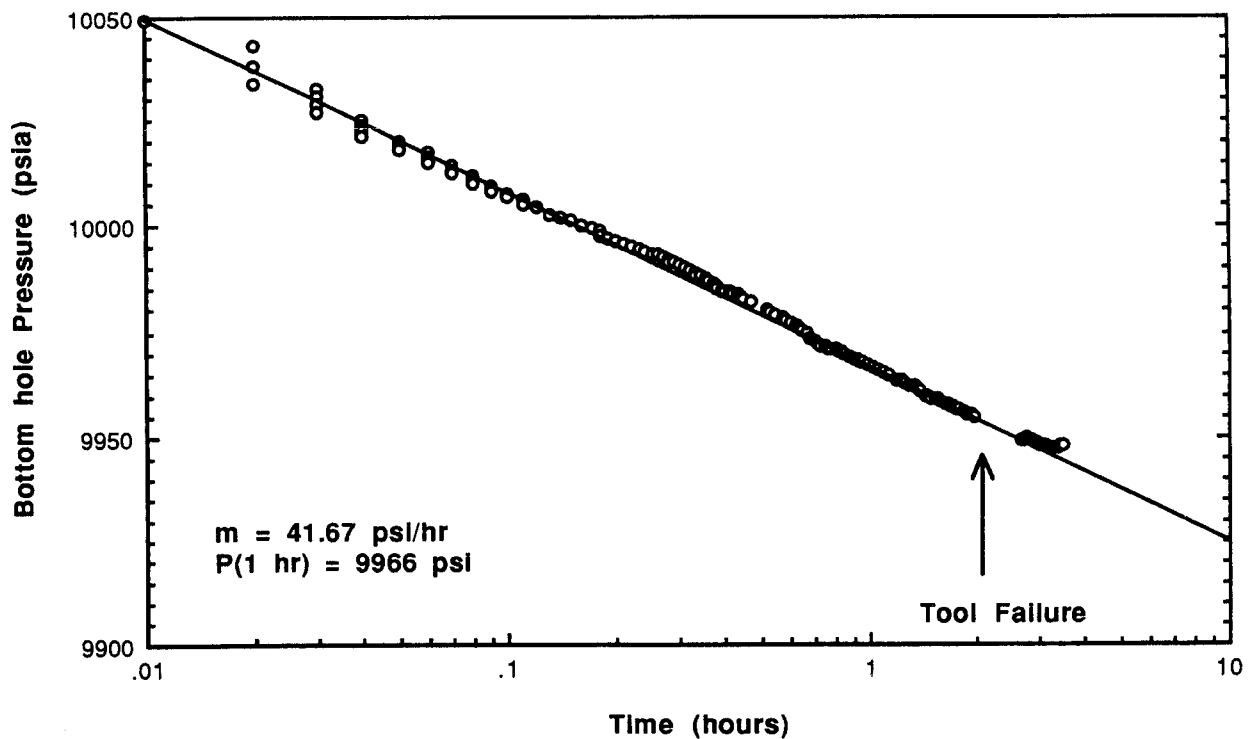

m = 41.67 psi/hr
P(1 hr) = 9966 psi

Tool Failure

Time (hours)

Figure A17. Apr 29-May 2 Buildup Test.

m1 = - 43.75 psi/cycle
P(1 hr) = 10084 psi

m2 = 96.67 psi/cycle
t-shutin = 14 hrs at intersection

Shutin Bottomhole Pressure (psi)

$(t + \Delta t) / \Delta t$